Winded Coils and Ferromagnetic Cores in Comsol Multiphysics (in progress)

Domenico Lahaye

November 13, 2009

Future Work on the 3D models

Extension of these notes

- animations
- visualization using COVISE

Chapter 1

Lumped Parameter Models of RL Circuits

Prior to detailing finite element models in subsequent chapters, we develop in this chapter simplified lumped parameter approximation that serve to get an intuitive feeling and point of comparison for the subsequent models. The point of departure for deriving lumped parameter models is the following first order ordinary differential equation relating the externally applied voltage excitation $V_e(t)$ with the current $I(t)$ in a circuit with an Ohmic resistance R and inductance L.

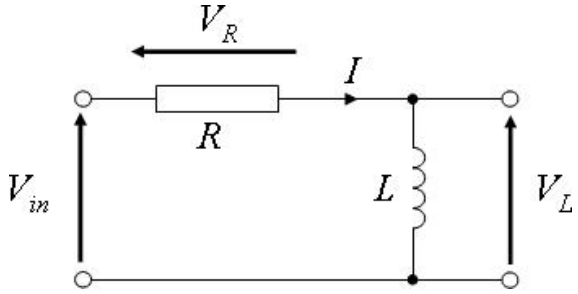

Figure 1.1: Series connection of a resistance and inductance.

$$V_R(t) + V_L(t) = V_{in}(t) \Leftrightarrow \frac{d}{dt}(L\,I) + R\,I = V_e(t)\,. \tag{1.1}$$

The terms in the left-hand side can be identified as the induced and resistive voltage, respectively, and the equation states that at all times the sum of the induced and resistive voltage is equal to the externally applied one. The equation needs to be supplied with an initial value for the current.

The Ohmic resistance R determined by the electrical conductivity of the medium. In the case that the coil is solenoid wounded N_t times around a ferromagnetic core with magnetic permeability μ, the impedance L can be expressed as

$$L = \mu\, N_t^2 \frac{S}{l_{path}} = \mu_0\, \mu_r\, N_t^2 \frac{S}{l_{path}}\,, \tag{1.2}$$

where S and l_{path} cross-section and length of the flux path in the ferromagnetic core respectively.

In this chapter we first derive an analytical expression for the current in an RL-circuit with *constant* impedance and two excitations: a constant and sinusoidally varying voltage source. These models illustrate how the presence of an impedance causes a phase shift in and amplitude reduction of the current. In more realistic models however the magnetic permeability μ of the core changes by moving the operation point on a non-linear B-H characteristic. In a second stage we therefore extend the model to include *changes* in the impedance induced by changes in the magnetic permeability. This model assumes the coil to be a solenoid for which expression (1.2) is correct. The generalisation of this model to more complex coil-core configurations is therefore not immediate.

Describe a mechanical equivalent: variable impedance and variable mass.

Goals In this chapter we aim at

- describing a simple model able to explain the inductive current limiting principle (including the concepts of induced voltage and phase difference between applied voltage and current). This simple model can possibly serve as coarse model inside an surrogate based optimisation algorithm.

- explaining why this simple model is not sufficient for the type of devices considered

To do:

1. describe drop in resistive voltage
2. describe presence of DC coil by additive constant in the flux

1.1 Ohmic Resistance of a Wire

Consider a cylindrical electrical conductor along the z-axis with length ℓ_z and cross-section Ω in the xy plane. The shape of the cross-section Ω is assumed to be z-independent. Consider furthermore a *stationary* electrical current flowing along the z-axis through the conductor. For stationary fields Faraday's law implies that the electric field $\mathbf{E}$ is curl free. This condition can be ensured by writing $\mathbf{E}$ in terms of the electric potential ϕ as

$$\mathbf{E} = -\nabla\phi\,. \tag{1.3}$$

Substituting this into Ohm's law $\mathbf{E} = \sigma\,\mathbf{J}$ yields

$$\mathbf{J} = -\sigma\,\nabla\phi\,. \tag{1.4}$$

For currents flowing in the z-direction only, the above relation yields

$$J_z = -\sigma\,\frac{\partial\phi}{\partial z}\,. \tag{1.5}$$

Assuming the gradient $\partial\phi/\partial z$ to be constant over the cross-section Ω, we obtain Ohm's law by integrating (1.5) over Ω in integral form

$$\triangle V = R\,I\,, \tag{1.6}$$

where

$$\triangle V = -\ell_z\frac{\partial\phi}{\partial z} \tag{1.7}$$

and

$$I = \int_\Omega J_z\,d\,\Omega \tag{1.8}$$

are the voltage drop over and the current through the conductor and where

$$R = \ell_z/\left(\int_\Omega \sigma\,d\,\Omega\right) \tag{1.9}$$

is the ohmic resistance of the conductor expressed in Ohm Ω. Equation (1.6) can be rewritten as

$$I = G\ \triangle V\,, \tag{1.10}$$

where

$$G = \frac{1}{R}\,, \tag{1.11}$$

is the conductance of the conductor.

1.2 Inductance of a Winded Coils

1.2.1 Definition

- give definition of (self and mutual) inductance
- give units (Henry) and function of primary units

$$1\mathrm{H} = 1\mathrm{Wb/A} = 1\mathrm{T\,m^2/A} = 1\frac{\mathrm{V\,s}}{\mathrm{m^2}}\mathrm{m^2/A} = 1\frac{\mathrm{V}}{\mathrm{A}}\mathrm{s} = 1\Omega\,\mathrm{s} \tag{1.12}$$

- give range of value for applications (tens of miliHenry)

1.2.2 Magnetic Flux

Considering the coil to be an interconnection of N_t flux contributions, the magnetic flux and the coil impedance are related by

$$\psi(t) = N_t\,\phi(t) = L(t)\,I(t) \Leftrightarrow L(t) = \frac{N_t\,\psi(t)}{I(t)} = \frac{\phi(t)}{I(t)}\,. \tag{1.13}$$

Assuming that $I(t) \neq 0$, this expression allow to compute the impedance via the magnetic flux.

1.2.3 Magnetic Energy

Consider that the volume Ω encloses the core and ferromagnetic core and has a permeability $\mu = \mu(\mathbf{x}, t)$. The magnetic energy W_m in Ω due to the magnetic flux $\mathbf{B}$ and field $\mathbf{H}$ induced due a time-varying current is given by the volume integral

$$W_m(t) = \frac{1}{2}\int_\Omega \mathbf{B}\cdot\mathbf{H}\,d\Omega = \frac{1}{2}\int_\Omega \mu\,\mathbf{B}\cdot\mathbf{B}\,d\Omega\,. \tag{1.14}$$

In a 2D perpendicular current formulation on a computational domain with cross-section Ω_{xy} in the xy-plane and length ℓ_z in the z-direction (examples will be given in subsequent chapters), this formula simplifies to the surface integral

$$W_m(t) = \frac{\ell_z}{2}\int_{\Omega_{xy}} \big[B_xH_x + B_yH_y\big]\,d\Omega = \frac{\ell_z}{2}\int_{\Omega_{xy}} \mu\big[B_xB_x + B_yB_y\big]\,d\Omega\,. \tag{1.15}$$

In case that the magnetic field is generated by a total current $I_{tot}(t)$ flowing through a coil with N_t windings and current $I(t)$ per turn, i.e., $I_{tot}(t) = N_t\,I(t)$, the magnetic energy and the coil impedance $L(t)$ are related by

$$W_m(t) = \frac{1}{2}L(t)I^2(t) \Leftrightarrow L(t) = 2\frac{W_m(t)}{I^2(t)}\,. \tag{1.16}$$

Not that the inductance scales

- *quadratically* with N_t;
- *linearly* with μ.

In case that μ is constant (no magnetic saturation), the impedance is current independent and can therefore be computed using any non-zero value for the current. In case that a sinusoidal current brings (a part of) the core alternatively in and out of saturation, the impedance can be computed for a particular working condition. In configurations in which different coils are present (AC and DC coil in the fault current limiter), the self-inductance of the coil can be computed by considering the current in the single coil only (setting the current in the other coils equal to zero).

1.3 Impedance

The Ohmic resistance of the wire and the inductance of a coil can be combined to form the total impedance denoted by X and defined by

$$X = \sqrt{R^2 + \omega^2 L^2}\,. \tag{1.17}$$

1.4 Constant Inductance Model

In this section we assume that $\frac{dL}{dt} = 0$. In this case, equation (1.1) reduces to

$$L\frac{dI}{dt} + R\,I = V(t)\,. \tag{1.18}$$

Given some initial condition, this ordinary differential equation can be solved numerically using a time-integrator taking a time-dependent resistance (simulation of fault) into account. In order to derive analytical expressions however, we assume from here on that $\frac{dR}{dt} = 0$. The ratio $\frac{R}{L}$ has the dimensions of an (angular) pulsation and will be denoted by ω_1 from here on. The solution of the homogeneous equation to (1.18) is

$$I_h(t) = C\exp(-R/L\,t) = C\exp(-\omega_1 t) \tag{1.19}$$

where C is chosen so to satisfy the initial conditions.

1.4.1 Constant Applied Voltage

In case that the applied voltage is constant and equal to V_0, the method of variation of constants yields that $I(t) = C(t)\, I_h(t)$, where

$$C'(t) = V_0/L \exp(\omega_1 t) \Rightarrow C(t) = V_0/L\, \omega_1 \exp(\omega_1 t) + C_0 = V_0/R \exp(\omega_1 t) + C_0\,. \tag{1.20}$$

For the current we then have

$$\begin{aligned} I(t) &= \big[V_0/R \exp(\omega_1 t) + C_0\big]\, \exp(-\omega_1 t) && (1.21)\\ &= V_0/R + C_0 \exp(-\omega_1 t)\,, && (1.22)\end{aligned}$$

where the integration constant C_0 is related to the initial condition $I(t=0) = I_0$ by

$$C_0 = I_0 - V_0/R\,. \tag{1.23}$$

The current is then given by

$$I(t) = \frac{V_0}{R} + \big[I_0 - V_0/R\big] \exp(-\omega_1 t)\,. \tag{1.24}$$

If the relaxation time $\tau = L/R$ is sufficiently small (i.e., if the resistance R is not too small and the inductance L is not too large), then after a few multiples of the relaxation time, the current is independent of the initial condition and equal to its stationary value

$$\boxed{I(t) = \frac{V_0}{R}\,.} \tag{1.25}$$

1.4.2 Sinusoidally Varrying Applied Voltage

In case that the applied is sinusoidally varying, i.e., $V(t) = V_0 \sin(\omega_0 t)$, the method of variation of constants yields that $I(t) = C(t)\, I_h(t)$, where

$$C'(t) = V_0/L \sin(\omega_0 t) \exp(\omega_1 t) \Rightarrow C(t) = (V_0/L) \int^t \sin(\omega_0 s) \exp(\omega_1 s)\, ds + C_0\,. \tag{1.26}$$

for some integration constant C_0. Applying integration by parts twice yields

$$\begin{aligned} L/V_0\, C(t) &= \big[1/\omega_1 \sin(\omega_0 s) \exp(\omega_1 s)\big]^t - \omega_0/\omega_1 \int^t \cos(\omega_0 t) \exp(\omega_1 s)\, ds + C_0 && (1.27)\\ &= 1/\omega_1 \sin(\omega_0 t) \exp(\omega_1 t) - \omega_0/\omega_1^2 \big[\cos(\omega_0 s) \exp(\omega_1 s)\big]^t && (1.28)\\ &\quad -\omega_0^2/\omega_1^2 \int^t \sin(\omega_0 s) \exp(\omega_1 s)\, ds + C_0 && (1.29)\\ &= 1/\omega_1 \sin(\omega_0 t) \exp(\omega_1 t) - \omega_0/\omega_1^2 \cos(\omega_0 t) \exp(\omega_1 t) && (1.30)\\ &\quad -\omega_0^2/\omega_1^2 \int^t \sin(\omega_0 s) \exp(\omega_1 s)\, ds + C_0 && (1.31)\end{aligned}$$

Hence

$$[1 + \omega_0^2/\omega_1^2]\, C(t) = 1/\omega_1 (V_0/L) \sin(\omega_0 t) \exp(\omega_1 t) - \omega_0/\omega_1^2 (V_0/L) \cos(\omega_0 t) \exp(\omega_1 t) + C_0 \tag{1.32}$$

or

$$\begin{aligned} C(t) &= (V_0/L)\big[\frac{\omega_1}{\omega_0^2 + \omega_1^2} \sin(\omega_0 t) - \frac{\omega_0}{\omega_0^2 + \omega_1^2} \cos(\omega_0 t)\big] \exp(\omega_1 t) + C_0 && (1.33)\\ &= \frac{V_0}{L(\omega_0^2 + \omega_1^2)} \big[\omega_1 \sin(\omega_0 t) - \omega_0 \cos(\omega_0 t)\big] \exp(\omega_1 t) + C_0 && (1.34)\\ &= \frac{V_0 \sqrt{\omega_0^2 + \omega_1^2}}{L(\omega_0^2 + \omega_1^2)} \big[\frac{\omega_1}{\sqrt{\omega_0^2 + \omega_1^2}} \sin(\omega_0 t) - \frac{\omega_0}{\sqrt{\omega_0^2 + \omega_1^2}} \cos(\omega_0 t)\big] \exp(\omega_1 t) + C_0 && (1.35)\\ &= \frac{V_0}{L\sqrt{\omega_0^2 + \omega_1^2}} \big[\sin(\omega_0 t) \cos\Theta - \cos(\omega_0 t) \sin\Theta\big] \exp(\omega_1 t) + C_0 && (1.36)\\ &= \frac{V_0}{X} \sin(\omega_0 t - \Theta) \exp(\omega_1 t) + C_0 && (1.37)\end{aligned}$$

where we've introduced the phase shift

$$\frac{\sin\Theta}{\cos\Theta} = \frac{\omega_0}{\omega_1} \Leftrightarrow \Theta = \arctan(\frac{\omega_0}{\omega_1}) = \arctan(\frac{2\pi\, f\, R}{L})\,, \tag{1.38}$$

and where the integration constant C_0 is related to the initial condition by

$$C_0 = I_0 - \frac{V_0}{X}\sin(\Theta)\,. \tag{1.39}$$

The current is then given by

$$I(t) = \frac{V_0}{X}\sin(\omega_0 t - \Theta) + \big[I_0 - \frac{V_0}{X}\sin\Theta\big]\exp(-\omega_1 t)\,. \tag{1.40}$$

If the relaxation time $\tau = 1/\omega_1 = L/R$ is suffuciently large, then after a few multiples of the relaxation time, the current is independent of the initial condition and equal to

$$\boxed{I(t) = \frac{V_0}{X}\sin(\omega_0 t - \Theta)\,.} \tag{1.41}$$

Compared with a purely resistive network, the current has both a lower amplitude and a phase shift. A large inductance in particular will lead to a lower current value and a larger phase shift. This is illustrated in Figure 1.4.2.

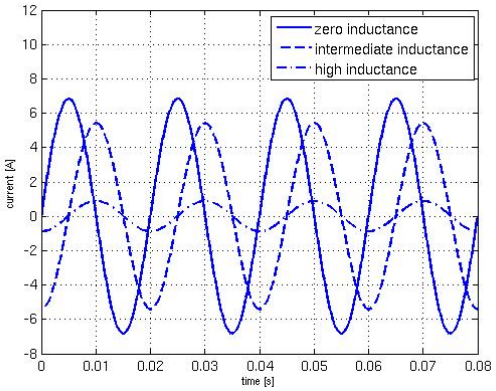

Figure 1.2: Current in RL-circuit for different values of the inductance.

1.5 Flux-Variable Inductance Model

The models developed in the previous section cease to be valid in situations in which the working point changes in time over a range in which the permeability and therefore the impedance can no longer assumed to be constant. The case that we will be interested in is the one in which the permeability varries along a non-linear B-H characteristic and which time-varrying voltage source bringing the ferromagnetic core in (low permeability and impedance) and out (high permeability and impedance) of saturation.

To extend our models to variable impedance cases, it turns out to be convenient to replace the current by the flux as state variable

$$\psi = L\, I \Leftrightarrow I = \frac{\psi}{L(\psi)} \tag{1.42}$$

and to rewrite the equation (1.1) modelling an RL-circuit as

$$\frac{d}{dt}\psi + \frac{R}{L(\psi)}\psi = V(t)\,. \tag{1.43}$$

In this model the variable impedance can be computed using the non-linear characteristic data assuming the model (1.2) for a solenoid. In this case we have that

$$L(\psi) = \mu\big[B(\psi)\big]N_t^2\frac{S}{l_{path}} \tag{1.44}$$

$$= \mu\big[\frac{\psi}{S}\big]N_t^2\frac{S}{l_{path}}\,. \tag{1.45}$$

Given an inital condition $\psi(t=0) = L(t=0)I(t=0)$, the ODE (1.43) can be solved numerical for the flux ψ and thus also for current I using (1.42).

This model extends the models of the previous section to a variable impedance and thus allow to illustrate the inductive fault current limiting effect. This model still has limited applicability as it uses the expression for the solenoid.

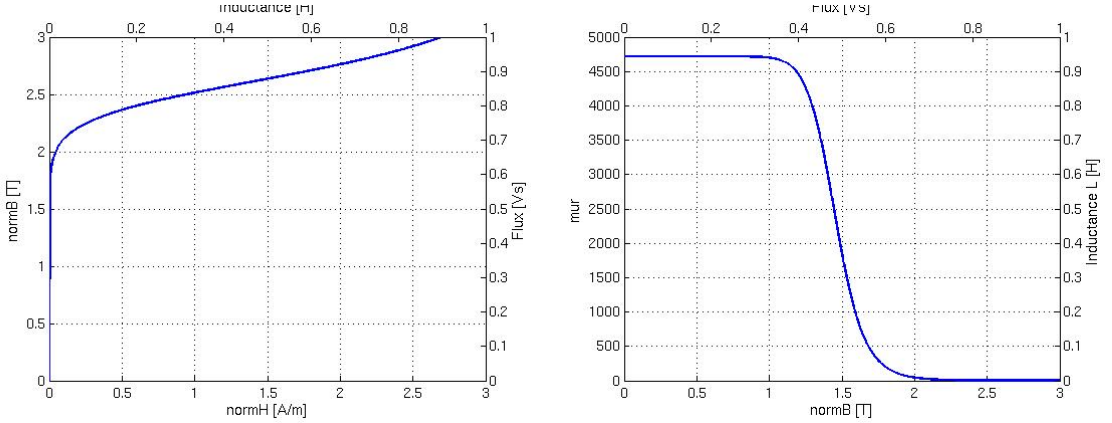

(a) B-H-curve (b) μ_r-B curve

Figure 1.3: Rational Function Approximation of the B-H curve.

1.6 Numerical Example

In this section we employ the model developed in the previous section to illustrate how a coil with a flux-variable impedance can work as a fault current limiter.

```
1  function [T,psi] = solve_rlcircuit(my_ctx)
2
3    %..Compute initial condition taking phase shift into account..
4    Rpre    = 5; Rpost = .1; R_init = Rpre+Rpost; Tfault = 1; Vmax = 28;
5    L_init  = lookup_imped(0,my_ctx);
6    om      = 2*pi*50;
7    X_init  = sqrt(R_init^2 + om^2*L_init^2);
8    phase_shift = atan(om*R_init/L_init);
9    I_init   = -Vmax/X_init*sin(phase_shift);
10   psi_init =  L_init*I_init;
11
12   %..Add DC component..
13   V_dc = -.4;
14   psi_dc = L_init*V_dc/R_init;
15
16   %..Solve ODE for the magnetic flux..
17   Tend    = 0.32;
18   options = odeset('RelTol',1e-12,'AbsTol',1e-12);
19 %  options = [];
20   [T,psi] = ode45(@rlcircuit,[0 Tend],psi_init+psi_dc,options);
21
22   function dpsidt = rlcircuit(t,psi)
23
24     if (t<Tfault) Rline = Rpre+Rpost; else Rline = Rpost; end
25     Vline  = V_dc + Vmax*sin(2*pi*50*t);
26     Limpd  = lookup_imped(psi,my_ctx);
27     dpsidt = Vline - Rline/Limpd*psi;
28
29     end
```

```
30
31    end
```

```
 1  function Limpd = lookup_imped(psi, my_ctx);
 2
 3    global Limpd
 4
 5    btopsi = my_ctx.btopsi;
 6    murtoL = my_ctx.murtoL;
 7    psi_dc = my_ctx.psi_dc;
 8
 9    %..Find b..
10    b = psi/btopsi;
11
12    %..Find relative permeability..
13    mur = bhcurve(b);
14
15    %..Find inductance..
16    Limpd = murtoL*mur;
17
18    %..Overwrite with an a-priori value
19    if (0)
20      Limpd = 1e-1;
21    end
```

```
 1  function mur = bhcurve(b)
 2
 3   %..BH curve definition..
 4   bha = 2.12e-4;
 5   bhb = 7.358;
 6   bhc = 1.18e6;
 7
 8   %..Define mur-b2 curve
 9   b2 = b.*b;
10   nur = bha + (1-bha)*b2.^bhb./(b2.^bhb+bhc);
11   mur = 1./nur;
12
13   %..If desired, overwrite with linear material..
14   if (0)
15     mur = ones(size(b));
16   end
```

Chapter 2

Quasi Stationary Magnetic Fields Models

- Maxwell equations including conservation of charge and the fact that $\nabla \cdot J = 0$ implies that the electrical charge density is time-independent
- magnetic constitutive relations including saturation, hysteresis and permanent magnets
- time-harmonic formulation: single and multiple frequencies
- boundary conditionings expressing symmetry (see e.g. team25)
- perpendicular current application mode including the expressions for the magnetic field and magnetic field density
- azimuthal current application model including derivation of the PDE using the curl in cylindrical coordinates, the boundary condtion expressing axial symmetry and things as above
- induced voltage - stranded conductor model - winding function: be careful on documenting the scaling with the coil cross-section
- induced current - eddy current losses
- magnetic force computation
- illustrations: voice-coil, team25, model of Firman and FCL

Remark Defining the induced voltage with bad sign may result in non-convergence of the transient simulation. In order to check the sign of the induced voltage, one can proceed as follows: run in a first stage a transient computation without the induced voltage in the ODE and check that the two ways of computing the induced voltage to match. Run in a second stage a transient computation with the induced voltage incorporated in the ODE.

2.1 Maxwell Equations

To add

- constitutive relations with permanent magnets
- conservation of charge $\frac{\partial \rho(\mathbf{x},t)}{\partial t} + \nabla \cdot \mathbf{J}(\mathbf{x},t) = 0$

The starting point for deriving partial differential equation models for magnetic field computations are the Maxwell equations [**?**, **?**]. These equations relate five vector fields: the magnetic field $\mathbf{H}$, the magnetic flux density (or induction) $\mathbf{B}$, the electric field $\mathbf{E}$, the electric displacement $\mathbf{D}$ and the electric current density $\mathbf{J}$. They can be written as

$$\nabla \times \mathbf{H} - \sigma\, \mathbf{v} \times \mathbf{B} = \mathbf{J} + \frac{\partial \mathbf{D}}{\partial t}\,, \tag{2.1}$$

$$\nabla \times \mathbf{E} = -\frac{\partial \mathbf{B}}{\partial t}\,, \tag{2.2}$$

$$\nabla \cdot \mathbf{B} = 0\,, \tag{2.3}$$

$$\nabla \cdot \mathbf{D} = \rho \,, \tag{2.4}$$

where ρ is the electric charge density and where $\mathbf{v}$ is the velocity of the medium with electrical conductivity σ. Equations (2.1) and (2.2) are Ampère's law and Faraday's law respectively. Equations (2.3) and (2.4) are conservation laws. The Maxwell equations have to be completed with constitutive material equations

$$\mathbf{B} = \mu \, \mathbf{H} \,, \tag{2.5}$$

$$\mathbf{D} = \epsilon \, \mathbf{E} \,, \tag{2.6}$$

$$\mathbf{J} = \sigma \, \mathbf{E} \,, \tag{2.7}$$

where μ, ϵ and σ are the magnetic permeability and the electric permittivity and conductivity respectively. Equations (2.5) and (2.6) are the magnetic and dielectric relations, and equation (2.7) is Ohm's law. In the general case, the quantities μ, ϵ and σ are tensors. Maxwell's equations can be derived from a minimising the electromagnetic energy

$$\begin{aligned} W_{tot}(t) &= W_e(t) + W_m(t) && (2.8) \\ &= \frac{1}{2} \int_\Omega \mathbf{D} \cdot \mathbf{E} \, d\Omega + \frac{1}{2} \int_\Omega \mathbf{B} \cdot \mathbf{H} \, d\Omega \,. && (2.9) \end{aligned}$$

In the following sections the full set of Maxwell equations are reduced to simpler models by making assumptions on the time-behavior of the field and the dimensions of the problem.

2.2 Magnetostatic Scalar and Vector Potential Formulation

In a stationary regime, the magnetic field quantities are decoupled from the electric ones and governed by

$$\nabla \times \mathbf{H} - \sigma \, \mathbf{v} \times \mathbf{B} = \mathbf{J} \,, \tag{2.10}$$

$$\nabla \cdot \mathbf{B} = 0 \,, \tag{2.11}$$

$$\mathbf{B} = \mu \, \mathbf{H} \,. \tag{2.12}$$

By introducing either a scalar or magnetic vector potential, these equations transform into second order partial differential equations. In the case that $\mathbf{v} = 0$, Equation (2.13) states that electrical charges moving uniformly in time give rise to a static magnetic field. If in addition $\mathbf{J} = 0$, then the curl-free condition for the magnetic field $\mathbf{H}$ (2.13) is ensured by expressing $\mathbf{H}$ in terms of the scalar magnetic potential V_m as

$$\mathbf{H} = \nabla V_m \,. \tag{2.13}$$

The substitution of (2.13) and (2.12) into (2.11) yields

$$\nabla \cdot (\mu \nabla V_m) = 0 \,. \tag{2.14}$$

The divergence-free condition for the for the magnetic flux density $\mathbf{B}$ (2.11) is ensured by expressing $\mathbf{B}$ in terms of the magnetic vector potential $\mathbf{A}$ as

$$\mathbf{B} = \nabla \times \mathbf{A} \,. \tag{2.15}$$

or

$$\begin{aligned} \mathbf{B} &= (B_x(x,y,z), B_y(x,y,z), B_z(x,y,z)) && (2.16) \\ &= \left(\frac{\partial A_z}{\partial y} - \frac{\partial A_y}{\partial z}, -\frac{\partial A_z}{\partial x} + \frac{\partial A_x}{\partial z}, \frac{\partial A_y}{\partial x} - \frac{\partial A_x}{\partial y} \right) . && (2.17) \end{aligned}$$

The substitution of (2.15) and (2.12) into (2.13) yields

$$\nabla \times (\nu \, \nabla \times \mathbf{A}) - \sigma \, \mathbf{v} \times (\nabla \times \mathbf{A}) = \mathbf{J} \,, \tag{2.18}$$

where $\nu = 1/\mu$ is the magnetic reluctivity. Equation (2.18) is a coupled system of three second order PDEs for the three components of $\mathbf{A}$. Once this system has been solved for $\mathbf{A}$, the technically relevant fields $\mathbf{B}$ and $\mathbf{H}$ can be calculated by relations (2.15) and (2.12).

To avoid the complexity of solving (2.18), two-dimensional approximations are often considered in engineering practice. We will consider two such approximations: a two dimensional Cartesian formulation and an axi-symmetrical formulation in cylindrical coordinates. In many applications, these formulations already give valuable information of the device under consideration.

2.2.1 Perpendicular Current Formulation

In two-dimensional Cartesian formulations, the problem is posed on a domain Ω lying in the xy-plane and all field quantities are assumed to be z-independent. Here Ω models for example the cross-section perpendicular to the axis of an electrical machine. The current density $\mathbf{J}$ is assumed to be perpendicular to Ω

$$\mathbf{J} = (0, 0, J_z(x, y)) \ . \tag{2.19}$$

Due to symmetry, the field quantity $\mathbf{B}$ lies in the plane Ω

$$\mathbf{B} = (B_x(x, y), B_y(x, y), 0) \ . \tag{2.20}$$

Condition (2.15) can therefore be met assuming a potential $\mathbf{A}$ of the form

$$\mathbf{A} = (0, 0, A_z(x, y)) \ . \tag{2.21}$$

and by (2.11) the components of $\mathbf{B}$ in can be expressed as

$$B_x = \frac{\partial A_z}{\partial y} \text{ and } B_y = -\frac{\partial A_z}{\partial x} \, . \tag{2.22}$$

By this assumption, the system (2.18) reduces to a single second order PDE for the z-component of the magnetic vector potential

$$-\frac{\partial}{\partial x}\left(\nu \frac{\partial A_z}{\partial x}\right) - \frac{\partial}{\partial y}\left(\nu \frac{\partial A_z}{\partial y}\right) + \sigma \, v_x \frac{\partial A_z}{\partial x} + \sigma \, v_y \frac{\partial A_z}{\partial y} = J_z \, . \tag{2.23}$$

2.2.2 Azimuthal Current Formulation

In an axi-symmetrical formulation in cylinder coordinates $(r,\, \theta,\, z)$, the domain Ω lies in the rz-plane and all field quantities are assumed to be θ-independent. In analogy to the Cartesian formulation, the applied current density is assumed to be perpendicular to Ω

$$\mathbf{J} = (0, J_\theta(r, z), 0) \ . \tag{2.24}$$

As before the field quantity $\mathbf{B}$ only has components in the modeling plane

$$\mathbf{B} = (B_r(r, z), 0, B_z(r, z)) \ . \tag{2.25}$$

Condition (2.15) can therefore be met assuming a potential $\mathbf{A}$ of the form

$$\mathbf{A} = (0, A_\theta(r, z), 0) \ . \tag{2.26}$$

and by (2.11) in cylindrical coordinates

$$\nabla \times \mathbf{F} = \left(\frac{1}{r}\frac{\partial F_z}{\partial \theta} - \frac{\partial F_\theta}{\partial z}, \frac{\partial F_r}{\partial z} - \frac{\partial F_z}{\partial r}, \frac{1}{r}\left[\frac{\partial (r F_\theta)}{\partial r} - \frac{\partial F_r}{\partial \theta}\right]\right) \tag{2.27}$$

the components of $\mathbf{B}$ in can be expressed as

$$\begin{aligned} B_r &= -r\frac{\partial}{\partial z}\left(\frac{A_\phi(r, z)}{r}\right) && (2.28)\\ &= -\frac{\partial A_\phi(r, z)}{\partial z} && (2.29) \end{aligned}$$

and

$$\begin{aligned} B_z &= r\frac{\partial}{\partial r}\left(\frac{A_\phi(r, z)}{r}\right) + 2\frac{A_\phi(r, z)}{r} && (2.30)\\ &= r\frac{1}{r}\frac{\partial A_\phi(r, z)}{\partial r} - r A_\phi(r, z)\frac{1}{r^2} + 2\frac{\partial A_\phi(r, z)}{r} && (2.31)\\ &= \frac{\partial A_\phi(r, z)}{\partial r} + \frac{\partial A_\phi(r, z)}{r} && (2.32)\\ &= \frac{1}{r}\left[\frac{\partial}{\partial r}(r A_\phi(r, z))\right] && (2.33)\\ &= \frac{1}{r}\left[A_\phi(r, z)) + r\frac{\partial}{\partial r} A_\phi(r, z)\right] && (2.34)\\ &= \frac{A_\phi(r, z)}{r} + \frac{\partial A_\phi(r, z)}{\partial r} && (2.35) \end{aligned}$$

The system (2.18) then reduces to the scalar equation

$$-\frac{\partial}{\partial r}\left(\frac{\nu}{r}\,\frac{\partial(r\,A_\theta)}{\partial r}\right)-\frac{\partial}{\partial z}\left(\nu\,\frac{\partial A_\theta}{\partial z}\right)+\sigma\,v_r\frac{\partial A_\theta}{\partial r}+\sigma\,v_z\frac{\partial A_\theta}{\partial z}=J_\theta\,. \tag{2.36}$$

The PDE in form (2.23) or (2.36) is the governing PDE for two-dimensional stationary magnetic field computations.

2.3 Transient Formulation

In order to derive the time-dependent magnetic field formulation, we eliminate the current density $\mathbf{J}$ and the displacement current $\mathbf{D}$ in the right-hand side of Ampère's law (2.1) using Ohm's law (2.7) and the dielectric relation (2.6) respectively. These manipulations yield

$$\nabla\times\mathbf{H}=\sigma\,\mathbf{E}+\epsilon\frac{\partial\mathbf{E}}{\partial t}\,. \tag{2.37}$$

We assume the electro-magnetic excitations, and thus also the induced electro-magnetic fields, to vary periodically in time with period T and with frequency $f=1/T$. We introduce the dimensionless variable $t'=t/T=f\,t$. By rewriting the time derivative in the right-hand of (2.37) in this dimensionless variable, we obtain

$$\nabla\times\mathbf{H}=\sigma\,\mathbf{E}+\epsilon\,f\,\frac{\partial\mathbf{E}}{\partial t'}\,. \tag{2.38}$$

We assume the time-variations to be *quasi-stationary*. This assumption is justified by the fact that in technically relevant simulations of electro-magnetic energy transducers a sufficiently large upper bound on the frequency is

$$f\le 10^4\ \text{Hz}\ . \tag{2.39}$$

For the electrically conducting media that we will consider, the electric conductivity σ and permeability ϵ lie in the ranges

$$\sigma\in[0,10^9]\,C^2\,N^{-1}\,m^{-2}\,s^{-1}\ \text{and}\ \epsilon\in[\epsilon_0,10\,\epsilon_0]\,, \tag{2.40}$$

where $\epsilon_0=8.85\,.\,10^{-12}C^2\,N^{-1}\,m^{-2}$ is the permittivity of vacuum. The above bounds on f, σ and ϵ allow us to neglect the contribution of the displacement current, i.e. the second term in the right-hand side of (2.38). Hence, we obtain

$$\nabla\times\mathbf{H}=\sigma\,\mathbf{E}\,. \tag{2.41}$$

In the presence of time-varying fields, the definition (2.15) for the vector potential $\mathbf{A}$ remains valid. Introducing $\mathbf{A}$ in the left-hand side of (2.41) yields

$$\nabla\times(\nu\,\nabla\times\mathbf{A})=\sigma\,\mathbf{E}\,. \tag{2.42}$$

By Ohm's law (2.7), this equation can be written as

$$\nabla\times(\nu\,\nabla\times\mathbf{A})=\mathbf{J}\,. \tag{2.43}$$

In the presence of time-varying fields, the integration of Faraday's law (2.2) yields

$$\mathbf{E}=-\nabla\phi-\frac{\partial\mathbf{A}}{\partial t}\,, \tag{2.44}$$

where the gradient of the electric potential $\nabla\phi$ is an integration constant. The contributions of the two terms in the right-hand side of (2.44) to the current distribution will be treated separately. Substituting (2.44) into the right-hand side of (2.7) yields

$$\mathbf{J}=\mathbf{J}_s+\mathbf{J}_e\qquad\mathbf{J}_s=-\sigma\,\nabla\phi\qquad\mathbf{J}_e=-\sigma\,\frac{\partial\mathbf{A}}{\partial t}\,, \tag{2.45}$$

where $\mathbf{J}_s$ and $\mathbf{J}_e$ are the source and induced (or eddy) current density respectively. Substituting (2.45) into the right-hand side of (2.42), we obtain the following partial differential equation for the vector potential

$$\sigma\,\frac{\partial\mathbf{A}}{\partial t}+\nabla\times(\nu\,\nabla\times\mathbf{A})=\mathbf{J}_s\,. \tag{2.46}$$

2.4 Time-Harmonic Formulation

Solving the PDE (2.46) numerically entails a time-stepping procedure of some kind. In practice, a great deal of useful information can already be gained by assuming that the electromagnetic fields vary sinusoidally in time. Assuming a pulsation $\omega = 2\pi f$, we can write a generic electro-magnetic quantity $F(\mathbf{x}, t)$ oscillating harmonically in time as

$$F(\mathbf{x}, t) = \Re[\, \widehat{F}(\mathbf{x}) \exp(j\omega t)\,], \tag{2.47}$$

where the magnitude $\widehat{F}$ is a complex-valued quantity consisting of a real and imaginary part $\Re[\widehat{F}]$ and $\Im[\widehat{F}]$ respectively. In a time-harmonic formulation, the PDEs (2.43) and (2.46) reduce to the following PDE for the amplitude $\widehat{\mathbf{A}}$ of the vector potential

$$\nabla \times (\nu \nabla \times \widehat{\mathbf{A}}) = \widehat{\mathbf{J}} \tag{2.48}$$

and

$$\nabla \times (\nu \nabla \times \widehat{\mathbf{A}}) + j\,\omega\sigma\,\widehat{\mathbf{A}} = \widehat{\mathbf{J}}_s \tag{2.49}$$

respectively. By a reasoning analogous to the derivation of equation (2.23), we reduce the system of coupled PDEs (2.48) and (2.49) to a scalar PDE. In the former case we obtain the Poisson equation

$$-\frac{\partial}{\partial x}\left(\nu \frac{\partial \widehat{A}_z}{\partial x}\right) - \frac{\partial}{\partial y}\left(\nu \frac{\partial \widehat{A}_z}{\partial y}\right) = \widehat{J}_z \tag{2.50}$$

while in the latter a Helmholtz equation with complex shift

$$-\frac{\partial}{\partial x}\left(\nu \frac{\partial \widehat{A}_z}{\partial x}\right) - \frac{\partial}{\partial y}\left(\nu \frac{\partial \widehat{A}_z}{\partial y}\right) + j\,\omega\,\sigma\,\widehat{A}_z = \widehat{J}_{s,z}\,, \tag{2.51}$$

where $\widehat{J}_{s,z}$ denotes the z-component of the source current density $\widehat{\mathbf{J}}_s$. Equations (2.50) and (2.51) are the governing PDEs for two-dimensional time-harmonic magnetic field formulations. In Section 2.6 we will argue which circumstances motivate the choice for either one of these equations.

In (2.47) we assumed a single frequency oscillatory behavior. In more advanced formulations a small set a discrete frequencies is taken into account. Such formulations are called *multi-harmonic* [**?**, **?**].

2.5 Conductor Models

To do

- extends this part to the transient case
- include text on the impedance

Time-varying currents in a conductor magnetically induce eddy currents and voltages trying to counteract their source. The current will redistribute in such a way that the current density is larger towards the cross-section boundaries. This effect is known as the skin-effect and characterized by the skin-depth. The skin-depth δ is typical length scale measuring the size of the second order term relative to the term of order zero in the PDE (2.51) and is defined as

$$\delta = \sqrt{\frac{1}{\pi f\,\sigma\mu}}\,. \tag{2.52}$$

It is represented schematically in Figure **??**. Technically speaking, about 60% of the current flows in the shaded area in this figure. Different conductor models are distinguished based on the ratio between the skin-depth and the conductor radius, i.e. on the importance of the skin-effect in modeling the conductor. In this thesis we will consider *solid* and *stranded* conductors. For both conductor models and for time-varying field, one obtains by substituting (1.7) into (2.45) the relation

$$\widehat{J}_z = \frac{\sigma}{\ell_z}\,\widehat{\triangle V} - j\,\omega\,\sigma\,\widehat{A}_z \tag{2.53}$$

or, equivalently,

$$\widehat{\triangle V} = \ell_z \left(\frac{\widehat{J}_z}{\sigma} + j\,\omega\,\widehat{A}_z\right)\,. \tag{2.54}$$

Subscripts sol and str will be used to indicate properties associated with the solid and stranded conductors respectively.

2.5.1 Solid Conductors

To add

1. the example in CMP
2. the proximity effect

A solid conductor is a massive bar of electrically conducting material with homogeneous cross-section Ω_{sol}. The radius of a solid conductor is large compared with the skin-depth δ. The variation of the current density over Ω_{sol} can therefore not be neglected. The magnitude of the voltage drop $\widehat{\triangle V}_{sol}$ in contrast is constant over Ω_{sol}.

Rotor bars in an induction machine are typically modeled as solid conductors.

To generalize (1.6) for time-harmonic fields in a solid conductor, we integrate both sides of (2.53) over Ω_{sol}. Using the the fact that $\widehat{\triangle V}_{sol}$ is constant over Ω_{sol}, we find

$$\widehat{I}_{sol} = G_{sol}\,\widehat{\triangle V}_{sol} - j\,\omega \int_{\Omega_{sol}} \sigma\,\widehat{A}_z\,d\Omega\,, \tag{2.55}$$

where

$$G_{sol} = \frac{1}{\ell_z}\int_{\Omega_{sol}} \sigma\,d\Omega \tag{2.56}$$

is the Ohmic resistance of the solid conductor (see also e.g. [**?**]).

2.5.2 Stranded Conductors

The cross-section of a stranded conductor Ω_{str} is the union of several conductors, each of them too small to be modeled individually. The skin-depth is large compared to the radius of the individual conductors, allowing the skin effect in the individual conductors to be neglected. The current density $\widehat{J}_z$ is assumed to be constant over Ω_{str}. Due to magnetically induced voltages, the variation of potential drop over Ω_{str} has to be taken into account. Compared with a solid conductor, the roles of current density and voltage drop are interchanged.

While the solid conductor is a physical entity, the stranded conductor is merely a convenient mathematical tool that allows one to model, for example, the windings in the stator of an induction machine or the coil of a transformer.

Assuming that the stranded conductor is made up of N_t conductors, each carrying a current $\widehat{I}_{str}$, the average current density is

$$\widehat{J}_z = \frac{N_t\,\widehat{I}_{str}}{S_{str}}\,, \tag{2.57}$$

where S_{str} is the area of Ω_{str}. The individual conductors forming the stranded conductor are assumed to be connected in series. By this assumption the potential difference $\widehat{\triangle V}_{str}$ over the latter is equal to the sum of the potential differences $\widehat{\triangle V}$ over the conductors. This sum is approximated by N_t times the average potential difference $\widehat{\triangle V}_{av}$ over an individual conductor

$$\widehat{\triangle V}_{str} = N_t\,\widehat{\triangle V}_{av}\,, \tag{2.58}$$

where

$$\widehat{\triangle V}_{av} = \frac{1}{S_{str}}\int_{\Omega_{str}} \widehat{\triangle V}\,d\Omega\,. \tag{2.59}$$

Substituting (2.54) into (2.59), taking into account that the current distribution (2.57) as well as the conductivity σ are constant over Ω, one obtains

$$\widehat{\triangle V}_{str} = R_{str}\,\widehat{I}_{str} + j\,\omega\,\frac{N_t\,\ell_z}{S_{str}}\int_{\Omega_{str}} \widehat{A}_z\,d\Omega\,, \tag{2.60}$$

see also e.g. [**?**, **?**], where

$$R_{str} = \frac{N_t^2\,\ell_z}{S_{str}}\int_{\Omega_{str}} \frac{1}{\sigma}\,d\Omega \tag{2.61}$$

is the Ohmic resistance of the stranded conductor. The insulation material surrounding the individual solid conductors and the air gaps between them can be taken into account by multiplying σ in (2.61) by a positive factor smaller than one. This factor is called the *slot fill* factor.

2.6 Induced Fields in Conductive Media

Relations (2.55) and (2.60) generalize Ohm's law (1.6) to time-harmonic currents. The first and second term of the right-hand side of (2.55) represent the resistive and inductive currents respectively . The two terms in the right-hand side of (2.60) are the resistive and inductive voltage . The relations (2.55) and (2.60) couple magnetic field quantities with integrated electric ones and are called *electrical circuit relations* .

To compute the magnetic field over the cross-section of a conductor, appropriate field equations and circuit relations have to be coupled. The right-hand side in PDE (2.51) can be written in terms of the applied voltage $\widehat{\triangle V}_{sol}$ over a solid conductor using (2.45) and (1.7)

$$\widehat{J}_{s,z} = -\sigma \frac{\partial \phi}{\partial z} = \frac{\sigma}{\ell_z} \widehat{\triangle V}_{sol} \,, \tag{2.62}$$

and is thus constant over Ω_{sol}. It is therefore convenient to choose the PDE (2.51) in the form

$$-\frac{\partial}{\partial x}\left(\nu \frac{\partial \widehat{A}_z}{\partial x}\right) - \frac{\partial}{\partial y}\left(\nu \frac{\partial \widehat{A}_z}{\partial y}\right) + j\,\omega\,\sigma\,\widehat{A}_z = \frac{\sigma}{\ell_z}\widehat{\triangle V}_{sol} \tag{2.63}$$

for the computation of the magnetic field over Ω_{sol}. By a similar argument the magnetic field over the cross-section of a stranded conductor Ω_{str} is modeled by PDE (2.50). Upon eliminating the current density by (2.57), this PDE becomes

$$-\frac{\partial}{\partial x}\left(\nu \frac{\partial \widehat{A}_z}{\partial x}\right) - \frac{\partial}{\partial y}\left(\nu \frac{\partial \widehat{A}_z}{\partial y}\right) = \frac{N_t}{S_{str}}\,\widehat{I}_{str} \,. \tag{2.64}$$

Conductors can be excited by either a voltage or a current source. If a solid conductor is operated by a voltage source, the source term in the PDE (2.63) is a known constant, and the PDE can be solved. If instead the solid conductor is current driven, the source in the PDE has to be calculated from the electrical circuit relation (2.55). In this case, the PDE and the circuit relation have to be solved simultaneously for the magnetic vector potential and the applied voltage. To compute the magnetic field distribution of a voltage driven stranded conductor, the PDE (2.64) and the circuit relation (2.60) have to be solved simultaneously for the vector potential and the applied current.

2.7 Induced Voltage by the Time Variation of the Magnetic Flux

The voltage induced the time-varrying magnetic flux is given by

$$V_{ind} = -N_t \frac{d\psi}{dt} \,, \tag{2.65}$$

where the minus sign is due to Lenz's Law. Using the flux-impedance relation (1.13) the above relation can be written as

$$V_{ind} = \frac{d}{dt}(LI) \,. \tag{2.66}$$

In case that $\frac{dL}{dt} = 0$, this formula reduces to

$$V_{ind} = L \frac{d}{dt}(I) \,. \tag{2.67}$$

The magnetic flux $\psi(t)$ passing through an oriented surface S with outward normal $\mathbf{n}$ is given by the surface integral

$$\psi(t) = \int_S \mathbf{B} \cdot d\mathbf{S} = \int_S \mathbf{B} \cdot \mathbf{n}\, dS \,. \tag{2.68}$$

In applications of this expression we are typically interested in, the surface $S = S_{core}$ typically denotes the cross-section of the ferromagnetic core perpendicular to the flux path. In a 2D perpendicular current formulation on the domain Ω_{xy}, the surface S_{core} is then a line piece perpendicular to the y-axis extending from $x = x_m$ to $x = x_M$, extruded by a length ℓ_z in the z-direction. Using the vector potential $\mathbf{A}$ ($\mathbf{B} = \nabla \times \mathbf{A}$) as unknown, the above

expression reduces to

$$\begin{aligned}
\phi(t) &= \int_{S_{core}} \mathbf{B}\cdot\mathbf{n}\, dS && (2.69)\\
&= \int_{S_{core}} B_y\, dx\, dz && (2.70)\\
&= -\int_{x_m}^{x_M} dx \int_{z_m}^{z_M} dz \frac{\partial A_z}{\partial x} \quad [B_y = -\frac{\partial A_z}{\partial x}] && (2.71)\\
&= -\ell_z \int_{x_m}^{x_M} dx \frac{\partial A_z}{\partial x} && (2.72)\\
&= -\ell_z \left[A_z(x = x_M, t) - A_z(x = x_m, t)\right] && (2.73)\\
&= \ell_z \left[A_z(x = x_m, t) - A_z(x = x_M, t)\right] . && (2.74)
\end{aligned}$$

In other applications S might consist of a component S_{core} in the core and a component S_{air} in air (refer to the open core FCL). In this we can write

$$\phi^{tot}(t) = \phi^{core}(t) + \phi^{air}(t) \approx \phi^{core}(t) \qquad \text{if} \qquad \phi^{air}(t) \text{ is small.} \tag{2.75}$$

In an azimuthal current application we have that ...

2.8 Induced Voltage by a Homogenezation Procedure

In this section we review a technique allowing to compute the induced voltage in winded coils (also referred to as *stranded conductors*) by integrating its density over the volume in 3D (cross-section in 2D) of the conductor.

2.8.1 Three Dimensional

Need to include pictures of the 3D coils
To compute the induced voltage in winded coils the introduction of the so-called *winding function* t turns out to be useful. This is a vector function such that the applied current density in the coil can be expressed as

$$\mathbf{J} = I\,\mathbf{t} \tag{2.76}$$

We next give two examples of winding functions. For a *cylindrical coil* in the xy-plane with with center in (x_0, y_0, z_0), cross-section S and number of turns N_t and excited by a current flowing in counter clock wise direction, we have that $\mathbf{t}(x, y, z) = \frac{N_t}{S}(t_x(x, y), t_y(x, y), 0)$ where

$$t_x(x, y) = \frac{-(y - y_0)}{\sqrt{(x - x_0)^2 + (y - y_0)^2}} \text{ and } t_x(x, y) = \frac{x - x_0}{\sqrt{(x - x_0)^2 + (y - y_0)^2}} . \tag{2.77}$$

For a *cuboidal coil* occupying the surface $\Omega = (x_0, y_0) + ([-D, D] \times [-W, W] \setminus [-d, d] \times [-w, w])$ in the xy-plane extruded in the z-direction excited by a current in counter clockwise direction, we have again that $\mathbf{t}(x, y, z) = \frac{N_t}{S}(t_x(x, y), t_y(x, y), 0)$ where

$$t_x(x, y) = \begin{cases} -\text{sgn}(y) \text{ if} |y - y_0| > \frac{w}{d}|x - x_0| \\ 0 \text{ otherwise} \end{cases} \text{ and } t_y(x, y) = \begin{cases} \text{sgn}(x) \text{ if} |y - y_0| \le \frac{w}{d}|x - x_0| \\ 0 \text{ otherwise} \end{cases} . \tag{2.78}$$

In both cases we have that

$$\nabla\cdot\mathbf{t} = 0 (\text{ and thus } \nabla\cdot\mathbf{J} = 0) \text{ and} \|\mathbf{t}\| = \frac{N_t}{S} . \tag{2.79}$$

By a homogenization procedure over the individual windings in the coil, the induced voltage can be computed by integrating the density defined by the dot product $\mathbf{t}\cdot\mathbf{E}$ over the volume of the coil

$$V_{ind} = \int_{\Omega_{coil}} \mathbf{t}\cdot\mathbf{E}\, d\Omega . \tag{2.80}$$

Combining with the previous result, we have that

$$\boxed{\frac{d}{dt}(LI) = -N_t \frac{d\psi(t)}{dt} = \int_{\Omega_{coil}} \mathbf{t}\cdot\mathbf{E}\, d\Omega .} \tag{2.81}$$

This relation is the basis for the field-circuit coupling modeling of a winded coil excited by a voltage source. In what follows we make the relation for the induced voltage more explicit in two-dimensional computations.

2.8.2 Two Dimensional Perpendicular Current

In a perpendicular current computation we assume the cross-section of a winded coil to consist of components $S_{coil,1}$ and $S_{coil,2}$, excited by a current in positive and negative z-direction, respectively. The induced can then be computed as as follows

$$\begin{aligned} V_{ind} &= V_{ind,1} + V_{ind,2} && (2.82)\\ &= \frac{N_t\,\ell_z}{S_{coil,1}} \int_{S_{coil,1}} E_z\,dS - \frac{N_t\,\ell_z}{S_{coil,2}} \int_{S_{coil,2}} E_z\,dS && (2.83)\\ &= \frac{N_t\,\ell_z}{S_{coil,1}} \int_{S_{coil,1}} \frac{\partial A_z}{\partial t}\,dS - \frac{N_t\,\ell_z}{S_{coil,2}} \int_{S_{coil,2}} \frac{\partial A_z}{\partial t}\,dS && (2.84) \end{aligned}$$

where the minus sign stems from the fact that the current flows in opposite directions in both sides of the coil.

2.8.3 Two Dimensional Azimuthal Current

In a azimuthal current computation we the induced voltage in a coil with cross-section S_{coil} can the expressed as

$$\begin{aligned} V_{ind} &= \frac{N_t}{S_{coil}} \int_{S_{coil}} 2\pi r\,E_\phi\,dS && (2.85)\\ &= \frac{N_t}{S_{coil}} \int_{S_{coil}} 2\pi r\,\frac{\partial A_\phi}{\partial t}\,dS && (2.86) \end{aligned}$$

2.9 Boundary Conditions

The partial differential equations introduced before need to be supplied with boundary conditions. In this work we will make use of homogeneous Dirichlet, Neumann and periodic boundary conditions. When used in combination with a conformal mapping technique, the latter allow the modeling of infinite domains.

2.9.1 Axial Symmetry

2.9.2 Symmetry Boundary Conditions

2.9.3 Periodic Boundary Conditions

Let Γ_1 and Γ_2 be two disjoint parts of the boundary of the computational domain as shown in Figure **??** on page **??** for example. Let n_1 and n_2 denote the outward normal on Γ_1 and Γ_2 respectively. Periodic boundary conditions connect both the vector potential and its normal derivative on Γ_1 and Γ_2. Periodic boundary conditions state that

$$A_z|_{\Gamma_1} = A_z|_{\Gamma_2} \tag{2.87}$$

$$\nu\,\frac{\partial A_z}{\partial n_1}|_{\Gamma_1} = -\nu\,\frac{\partial A_z}{\partial n_2}|_{\Gamma_2}\,. \tag{2.88}$$

Anti-periodic boundary conditions state that

$$A_z|_{\Gamma_1} = -A_z|_{\Gamma_2} \tag{2.89}$$

$$\nu\,\frac{\partial A_z}{\partial n_1}|_{\Gamma_1} = \nu\,\frac{\partial A_z}{\partial n_2}|_{\Gamma_2} \tag{2.90}$$

see e.g. [**?**, **?**]. By imposing periodic boundary conditions one is able to reduce the area of the computational domain. We illustrate this point by an example. Consider the four-pole alternating current machine depicted in Figure **??** on page **??**. Due to symmetry in field and geometry, it is sufficient to model only two, or even just one pole of the machine. Figure **??** shows a two-pole half model of the motor being considered. In this model periodic boundary conditions relate the values on the straight edges at the bottom of the model. In the one-pole quarter model shown in Figure **??**, anti-periodic boundary conditions relate the values of the vertical and horizontal straight edge.

The reduction of the computational domain entails a saving in computational resources required to solve the problem or allows to obtain higher accuracy for the same problem size.

2.9.4 Unbounded Domains

In some practical magnetic field computations the domain Ω is unbounded. Different types of so-called *open boundary problems* exist. In a first one the accurate estimation of the field in a region of interest might require taking the surrounding unbounded domain into account. In a second type one is interested in far field effects, i.e. in the strength of the field at a large distance from the source. An example of the former is the computation of the magnetic field in the vicinity of a transformer. An example of the latter is the computation of the magnetic field excited by high voltage lines at ground level.

In numerical computations the unbounded domain needs to be truncated somehow. An overview of truncation techniques proposed in the literature can be found in [**?**].

In the application software considered in this work, a conformal mapping technique is used. To describe this technique formally, consider equation (2.23) posed on the domain $\Omega = \mathbb{R}^2$. The PDE has to be supplied with the condition that the potential remains finite at infinity. By properly scaling the potential, one can assume the value at infinity to be zero, i.e.

$$A_z(x,y) \to 0 \qquad \text{as } \sqrt{x^2+y^2} \to \infty\,. \tag{2.91}$$

The part of Ω that is of interest is enclosed in a disk Ω_D centered in $(0,0)$. The radius ρ of Ω_D is required to be large enough so that the source term J_z is zero on $(\Omega_D)^c = \mathbb{R}^2 \setminus \Omega_D$. We further assume ν to be constant on $(\Omega_D)^c$. Hence, the function A_z satisfies the Laplace equation on $(\Omega_D)^c$. Let A_D and A_{D^c} denote the restriction of A_z to Ω_D and $(\Omega_D)^c$ and n_D and n_{D^c} the outward normal on Ω_D and $(\Omega_D)^c$ respectively. The original problem on $\mathbb{R}^2$ is equivalent with

$$\begin{aligned} -\frac{\partial}{\partial x}\left(\nu\,\frac{\partial A_D}{\partial x}\right) - \frac{\partial}{\partial y}\left(\nu\,\frac{\partial A_D}{\partial y}\right) &= J_z \qquad \text{on } \Omega_D \\ -\frac{\partial^2 A_{D^c}}{\partial x^2} - \frac{\partial^2 A_{D^c}}{\partial y^2} &= 0 \qquad \text{on } (\Omega_D)^c\,, \end{aligned} \tag{2.92}$$

supplied with conditions ensuring the continuity of A_z and its normal flux across the boundary $\partial\Omega_D$. These continuity conditions can be stated as

$$A_D|_{\partial\Omega_D} = A_{D^c}|_{\partial\Omega_D} \qquad \text{and} \qquad \nu\,\frac{\partial A_D}{\partial n_D}|_{\partial\Omega_D} = -\nu\,\frac{\partial A_{D^c}}{\partial n_{D^c}}|_{\partial\Omega_D}\,. \tag{2.93}$$

After setting $z = x + j\,y$, one applies the conformal mapping

$$\mathcal{F}(z) = 1/z \tag{2.94}$$

to $(\Omega_D)^c$. The latter is mapped onto a disk Ω_E with radius $1/\rho$

$$\mathcal{F}[(\Omega_D)^c] = \Omega_E\,. \tag{2.95}$$

Properties of conformal transformations imply that the function A_{D^c} is a harmonic function on the image disk Ω_E if A_{D^c} is harmonic on the domain $(\Omega_D)^c$. The conformal mapping thus transforms the differential problem (2.92)-(2.93) into

$$\begin{aligned} -\frac{\partial}{\partial x}\left(\nu\,\frac{\partial A_D}{\partial x}\right) - \frac{\partial}{\partial y}\left(\nu\,\frac{\partial A_D}{\partial y}\right) &= J_z \qquad \text{on } \Omega_D \\ -\frac{\partial^2 A_{D^c}}{\partial x^2} - \frac{\partial^2 A_{D^c}}{\partial y^2} &= 0 \qquad \text{on } \Omega_E \end{aligned} \tag{2.96}$$

supplied with the conditions

$$A_D|_{\partial\Omega_D} = A_{D^c}|_{\partial\Omega_E} \quad \text{and} \quad \nu\,\frac{\partial A_D}{\partial n_D}|_{\partial\Omega_D} = -\rho^2\,\nu\,\frac{\partial A_{D^c}}{\partial n_E}|_{\partial\Omega_E}\,, \tag{2.97}$$

where n_E denotes the outward normal on Ω_E. The factor ρ^2 appearing in (2.97) is due to the local magnification $1/|\mathcal{F}'|$ evaluated on $\partial\Omega_D$ by conformal mapping. Using a conformal mapping we have thus transformed the original unbounded domain problem into two problems on bounded domains: a Poisson type problem on Ω_D and a Laplace problem on Ω_E. The condition (2.91) is assured by imposing the potential to be zero in the center of Ω_E

$$A_z = 0 \qquad \text{in center of } \Omega_E\,. \tag{2.98}$$

Chapter 3

Magnetic Saturation

In this section we describe the modeling of magnetic saturation in ferromagnetic materials, i.e., the modeling of the non-linear constitute relation between the magnetic flux $\mathbf{B}$ (units T) and the magnetic field $\mathbf{H}$ (units A/m). Using a vector potential formulation and denoting by $B = \|\mathbf{B}\|$, $H = \|\mathbf{H}\|$, the magnetic material law typically considered is

$$H(B) = \nu\, B = \nu_0\, \nu_r(B)\, B \Leftrightarrow \nu(B) = \frac{dH}{dB}(B)\,, \tag{3.1}$$

where ν_0 and ν (ν_r) denote the reluctivity of vacuum and the material (relative reluctivity), respectively [see paper Herbert on differential vs. chord reluctivity]. The inverse of the reluctivity is the permeability μ. Using a vector potential formulation, we have that

$$\|B\|^2 = \left(\frac{\partial A_z}{\partial y} - \frac{\partial A_y}{\partial z}\right)^2 + \left(-\frac{\partial A_z}{\partial x} + \frac{\partial A_x}{\partial z}\right)^2 + \left(\frac{\partial A_y}{\partial x} - \frac{\partial A_x}{\partial y}\right)^2 \tag{3.2}$$

Magnetic saturation is such that $\mu_r(B)$ is large and almost constant for small values of B and small almost constant for large values of B and has a non-linear transition between these two extreme values (see for instance Figure xxx).

In practise engineering practise, the function $\nu_r(B)$ is to be constructed from measured B-H samples. This process makes the convergence of an FEM computation prone stagnation. We therefore consider analytical expressions allowing to describe the function $\nu_r(B)$ analytically.

Goals In this chapter we aim at

- giving different analytical expressions for the non-linear B-H -curve modelling magnetic saturation
- give an example of a measured B-H
- illustrate a least square curve fitting technique allow to match the analytical expressions to the given measured data

To do

- add reference to rational BH-curve approximation
- add reference to Pechstein on approximating the BH-curve

3.1 Analytical Models

To do:

- make all plots of the BH-curves again
- compute the second derivative of the analytical model to see where the curvature changes from positive to negative.
- give a plot on double axis and deduce for which value of the current the core is in saturation.

3.1.1 Rational Function Approximation

In [1] the following rational expression modelling the relative reluctivity is given (denoting by $B = \|\mathbf{B}\|$)

$$\nu_r = a + \frac{(1-a)B^{2b}}{B^{2b}+c} \Leftrightarrow \mu_r = \frac{1}{a + \frac{(1-a)B^{2b}}{B^{2b}+c}} \tag{3.3}$$

where the values for the parameters a, b and c are given in Table 3.1. For this models holds that

$$\nu_r(B=0) = a \tag{3.4}$$

and thus the relative permeability at $B = 0$ is given by $1/a$ and that

$$\lim_{B\to\infty} \nu_r(B) = 1 \tag{3.5}$$

and thus the permeability never becomes smaller than μ_0 (which is physically correct).

a	2.12e-4
b	7.358
c	1.18e6

Table 3.1: Constants Used in the Rational Approximation

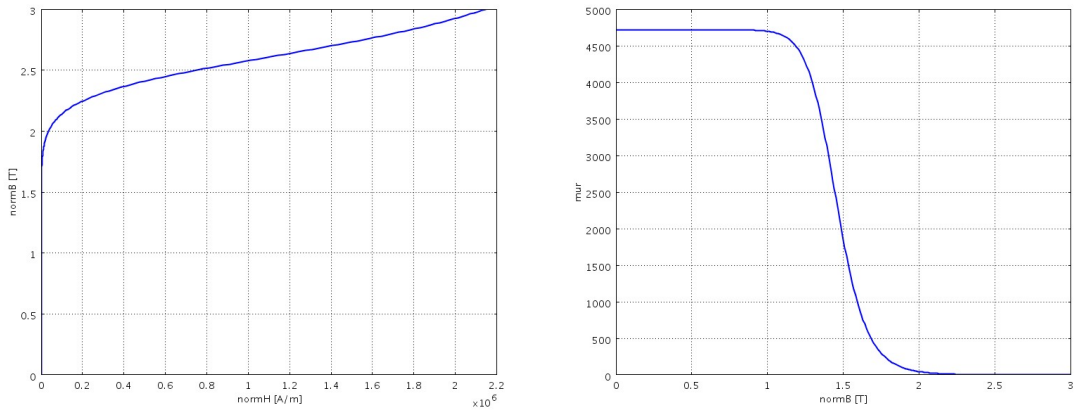

(a) B-H-curve

(b) μ_r-B curve

Figure 3.1: Rational Function Approximation of the B-H curve.

3.1.2 Hyperbolic Function Approximation

In [2] the following approximation is given:

$$B = C_1 \operatorname{arcsinh}(C_2 H) \Leftrightarrow H = \frac{1}{C_2}\sinh(\frac{B}{C_1}) \tag{3.6}$$

where the values for the parameters C_1 and C_2 are given in Table (3.2). From this we obtain the chord permeability

$$\mu = \frac{B}{H} = \frac{C_2 B}{\sinh(\frac{B}{C_1})} \tag{3.7}$$

$$\mu_r = \frac{\mu}{\mu_0} = \frac{C_2 B}{\mu_0 \sinh(\frac{B}{C_1})} \tag{3.8}$$

and the differential permeability

$$\nu = \frac{dH}{dB} = \frac{\cosh(C_2 B)}{C_1 C_2} \tag{3.9}$$

$$\mu = \frac{1}{\nu} = \frac{C_1 C_2}{\cosh(C_2 B)} \tag{3.10}$$

$$\mu_r = \frac{\mu}{\mu_0} = \frac{C_1 C_2}{\mu_0 \cosh(C_2 B)} \tag{3.11}$$

$$\tag{3.12}$$

As in this model

$$\lim_{B2 \to \infty} \mu_r(B2) = 0\,, \tag{3.13}$$

is has to be used with due care.

Remark This model requires a non-zero initial guess during intial guess to avoid the singularity at $B = 0$.

C_1	.25 [T]
C_2	.06 [m/A]

Table 3.2: Constants Used in the Sinh Approximation

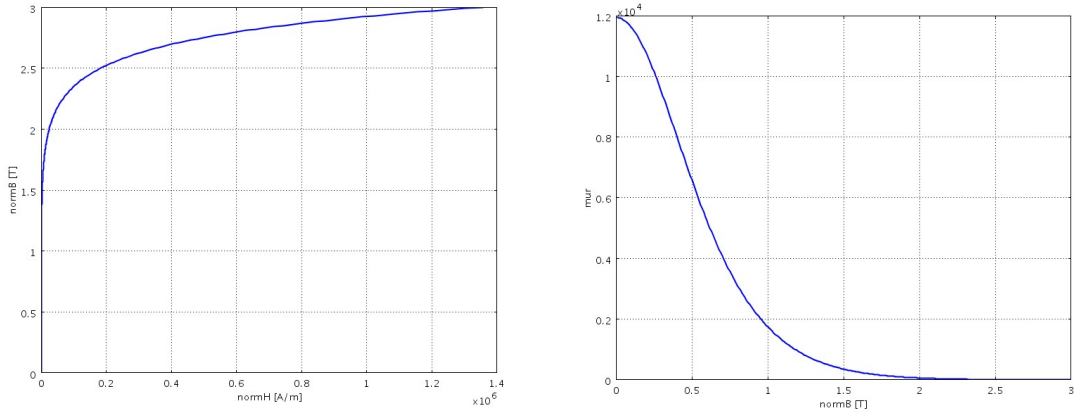

(a) B-H-curve (b) μ_r-B curve

Figure 3.2: Hyperbolic Function Approximation of a B-H curve.

3.2 Measured Data

In this section we give the measured B-H-data we will use in our numerical examples in subsequent chapters.

3.2.1 Measured BH data

```
H = [0 310      315     320     330     350     380     410     430 ...
470     500     540     580     620     650     670     720     750 ...
770     820     900     1000    1100    1200    1400    1800    2300 ...
2800    3300    4300    5300    8300    10300   15300   20300   25300 ...
30300   40300   50300   70300   100300  200300  400300  600300  800300 ...
1000300];

B = [0 1.3449   1.3773  1.4003  1.4328  1.4736  1.5112  1.5367  1.5501 ...
1.5715  1.5845  1.5991  1.6114  1.6221  1.6293  1.6337  1.6439  1.6494 ...
1.6529  1.661         1.6724    1.6847  1.6954  1.7048  1.7209  1.7457 ...
```

```
1.7687  1.7866  1.8012  1.8242  1.842   1.8796  1.8975  1.9299  1.9529 ...
1.9708  1.9854  2.0084  2.0262  2.0532  2.0817  2.1371  2.1926  2.225  ...
       2.248   2.2659 ];
```

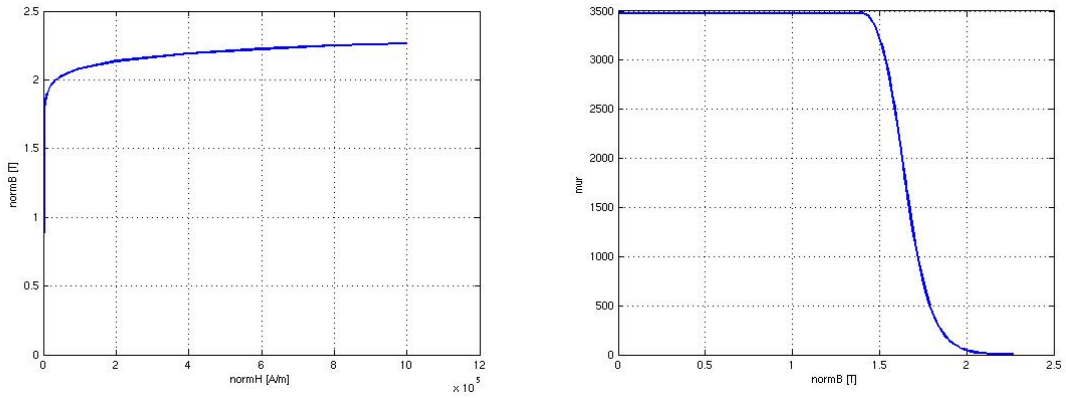

(a) B-H-curve (b) μ_r-B curve

Figure 3.3: B-H-curve used in tabular form.

3.3 Tuning the Analyical Models

In this section we performs a fitting of the parameters in the rational and hyperbolic approximation to the measured data by a non-linear optimisation procedure.

3.4 Further Extension

1. Make graphs of the derivative of μ_r wrt normB for the analytical and tabular data models. These graphs should how why the tabular is more difficult to work with.

3.5 Non-Convergence of the Non-linear Iteration during a Time-Stepping Procedure

During our extentive numerical testing with Comsol Mulphysics, we often encountered difficulties in making the non-linear iteration within the time-stepping procedure converge. Such difficulties are sometimes good to have as they point towards an erroneous problem formulation. Sometimes these errors come as a nuisance. In discussing strategies to overcome these difficulties we distinguish between non-convergence at the initial time step ($t = 0$) and non-convergence later in the time stepping procedure ($t > 0$).

3.5.1 Non-Convergence of the Initial Time Step

Often non-convergence of the initial time step can be cured by providing a better initial guess. An approach that we found fruitfull is to generate this initial guess using a seperate FEM computation.

3.5.2 Non-Convergence of Later in the Time Stepping Procedure

1. use anyltical BH-curve: limited flexibility
2. use tabular data: hard to obtain curve that is sufficiently smooth

3.5.3 For Me Open Issues

1. what is the effect of bad analytical approximation of the BH-curve, in particular in underestimating the slope in the initial part of the BH-curve
2. what do other commeercial FEM packages (Maxwell, ANSYS) do?

Chapter 4

Things to add

- hysteresis modeling and permanent magnets
- force computations
- iron and copper losses (see notes on safety transformer)
- modeling of motion and ALE formulation
- nodal FEM for double curl equation

Chapter 5

FEM Computations of Inductance and Induced Voltage

5.1 Axi-Symmetrical Models

The following experimental data was provided to us by Johan Wolmarans.

1. Coil 1 (larger)
   - Inductance at 50Hz: 4.6mH
   - Turns: approximately 192, wound in 4 layers
   - Wire diameter: 1mm
   - Wound around 110mm diameter (55mm radius) pipe
   - Coil height: 60mm
2. Coil 2 (as used to measure the carbon fiber sleeve)
   - Inductance at 50Hz: 615uH
   - Turns: 81, wound in 1 layer
   - Wire diameter: 1mm
   - Wound around 118mm diameter (59mm radius) pipe
   - Coil height: 90mm

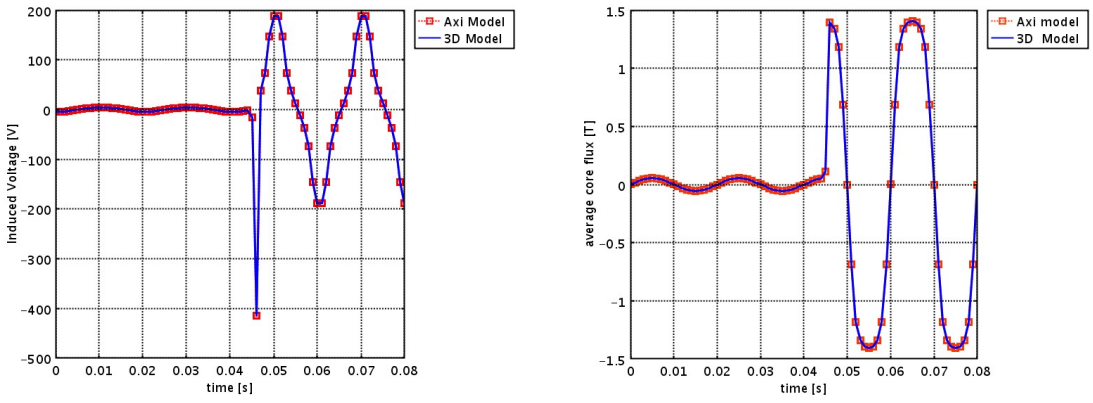

(a) Induced voltage

(b) Average magnetic flux

Figure 5.1: Axi-symmetrical and 3D computation of the induced voltage and magnetic flux.

5.2 Three Dimensional Models

	L (mH)	pre fault (A)	post fault (A)
axi-symmetrical	3.39	4.55	16.58
cylindrical	3.24	4.59	16.87
cuboidal	4.51	4.51	14.00
cuboidal with open core	17.29	3.44	5.01

Table 5.1: Values of inductance, pre and post fault current in different configurations.

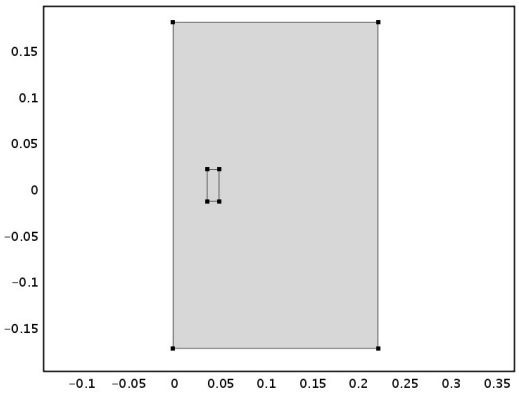

(a) Axi-symmetrical Model Geometry

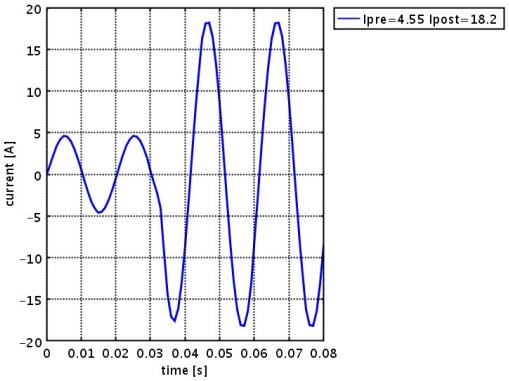

(b) Axi-symmetrical Model Current

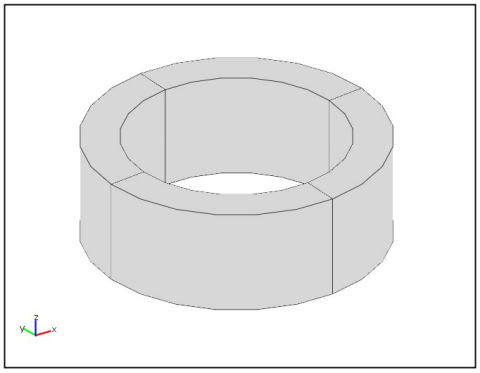

(c) Cylindrical Model Geometry

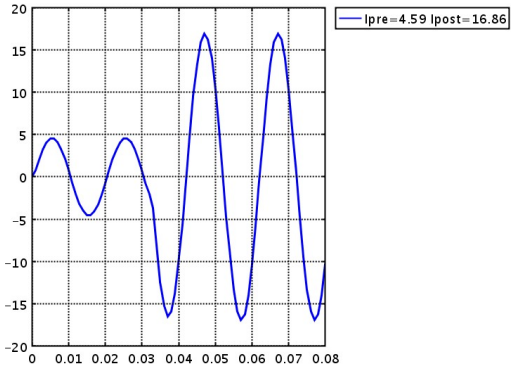

(d) Cylindrical Model Current

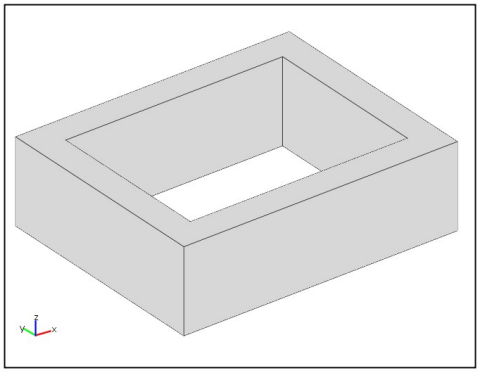

(e) Cuboidal Model Geometry

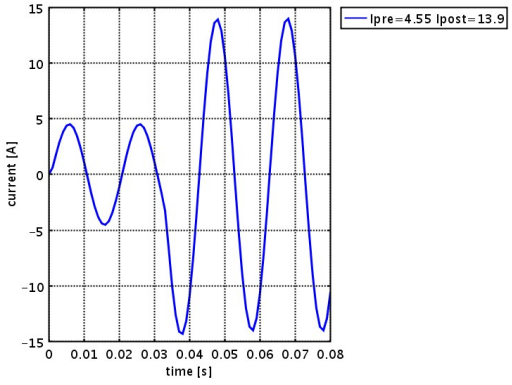

(f) Cuboidal Model Current

Figure 5.2: Different coil configurations and associated current waveforms.

Chapter 6

Two Dimensional FE Models of Inductive Fault Current Limiters

6.1 TO DO

1. in the first model
    - choice of surface S motivated by desire to minimize influence of fringing and leakage flux
    - investigate influence influence of space between coil and core
    - investige influence of gap in the core
    - describe three stage process in solving the model
    - include impedance computation after the second stage
    - describe the setting of the initial guess in assembling the first jacobian (different from jacobian specified in femsolver!)
2. additional model
    - open core model
    - three legs model

Goals

- simulate RL-circuit without having to resort analytical model for the impedance
- compute the impedance of a given configuration in three different ways, using the analytical formula, the magnetic energy and the magnetic flux
- compute the current waveform using only the AC coil, the DC coil in two different polarities and with linear and non-linear core
- check the magnetic flux density in the core legs and verify using the BH-curve to what extend the DC coils brings the legs in saturation
- investigate to what extend an ODE model allows to simulate this configuration, eventually by first computing the impedance
- investigate to what extend the geometry of the coils affects the current waveforms
- document issues on time integration

6.2 Introduction

To do:

- give a definition of the induced voltage in 3D (using the winding function), and show how it simplifies to perpendicular and azimuthal current application

In these notes we develop a sequence of numerical models of increasing accuracy and complexity for the current in coils winded around ferromagnetic cores. We start by detailing analytical and semi-analytical models, build two-dimensional finite element methods and extend these into three dimensions. Modelling results for the current wave forms are compared with laboratory measuments on scale models of the devices under study. Initially we were motivated by comparing different configurations of so-called inductive fault current limiters. The study of these devices was presented at the Comsol Multiphysics Users Conference 2008 in Hannover (+ reference). The configurations we study are however representative for a wide range of other applications in AC/DC modelling such as electrical machines, transformers and actuators. We therefore decided to document the solution to different difficulties we encountered in the modelling in Comsol Multiphysics, hoping that you (the reader) might learn from it.

6.3 Inductive Fault Current Limiters

Wikipedia defines a fault Current Limiter (FCL) to be a device which limits the prospective fault current when a fault occurs. Different types exist. The fault current limiter we consider here is based on an inductor and consists of a ferromagnetic core and two coils (see Figure xxx). We will refer to the coils as the AC and DC coils. The AC coil carries the line current. The DC coil provides the magnetic field on which the working principle of the FCL under consideration is based. It's working principle is detailed in [**?**] and can be summarized as follows:

- **nominal regime**: a time-independent current in the DC coil bring the core in saturation. A sinusoidal line current flows throught a wire represented by the the AC winding. Parameters (ohmic resistance of the wire) are such that the left and right core leg do not desaturate, i.e., the impedance of the left and right core leg remain small.
- **occurence of fault**: in case of fault, the drop in the ohmic resistance in the AC coil is compensated by the magnetically induced fields in the core, i.e., by the raise of the impedance of the coil. The particular construction of the FCL such that for $0 \leq t \leq T/2$ (where T denotes the period of the sinusoidal exitation of the AC coil) one of the core legs desaturates, causing the impedance (and thus the induced voltage) to raise and thus the current to be limited. During this period the other core leg remains in saturation,. i.e., it does not contribute to the limiting process. During the period $T/2 \leq t \leq T$, the role of the left and right core leg are inverted, meaning that over the whole period T sufficient limiting is guaranteed.

6.4 Half Period Limiter

6.4.1 Geometry

In defining the geometry the core acts master and the coil as slaves. This corresponds to the fact that the coils are wounded around the core.

1. **the core**:
   (a) core variables

```
crwin = 12.5e-3; crwout =  37.5e-3; crwleg = crwout - crwin;
crhin = 39e-3; crhout = 63e-3;
rad = 3e-3;
```

   (b) core:

```
core = fillet(rect2(-crwout,crwout,-crhout, crhout), 'radii', rad) ...
                        - rect2(crwin,crwin,-crhin,crhin);
```

2. **flux integration lines**:
   (a) **left core leg**: line from (-crwout,0) to (-crwin,0)

Figure 6.1: Open-core configuration.

```
fluxline1 = line1([-crwout,-crwin],[0,0]);
```

(b) **right core leg**: line from (crwin,0) to (crwout,0)

```
fluxline2 = line1([crwin,crwout],[0,0]);;
```

3. **the AC coil**:

   (a) AC coil variables

```
accoilw = 10e-3; accoilh = 20e-3;
xspacer =  2e-3
accoilradin = crlegw/2+xspacer; accoilradout = accoilradin+accoilw;
coilxc = crwin+crwleg/2;
```

   (b) AC coil:

```
accoil_right = rect2(accoilradin,accoilradout,-accoilh/2,accoilh/2);
accoil       = accoil_right+move(accoil_right,-2*accoilradin-accoilw,0);
accoil       = move(accoil,accoilxc,0);
```

4. **the DC coil**:

   (a) DC coil variables

```
dccoilh     = 10e-3; dccoilw = crwin/2;
dccoilradin = (crhout-crhin)/2; dccoilradout = dccoilradin + dccoilh;
dccoilyc    = crhin+(crhout-crhin)/2;
```

   (b) DC coil

```
dccoil_top  = rect2(-dccoilw/2,dccoilw/2,dccoilradin,dccoilradout);
dccoil      = dccoil_top + move(dccoil_top,0,-2*dccoilradin-dccoilh);
dccoil      = move(dccoil,0,dccoilyc);
```

5. **the air**:

Figure 6.2: Three legged core configuration.

(a) air variables

```
airh = 400e-3; airw = 400e-3
```

(b) `air = rect2(-airh, airh, -airw, airw);`

The 1D and 2D entities in the geometry are then combined using

```
clear c s
c.objs={fluxline1,fluxline2};
c.name={'fluxline1','fluxline2'};
c.tags={'g5','g6'};

s.objs={air,accoil,dccoil,core};
s.name={'air1','accoil','dccoil','core'};
s.tags={'g1','g2','g3','g4'};

fem.draw=struct('c',c,'s',s);
fem.geom=geomcsg(fem);
```

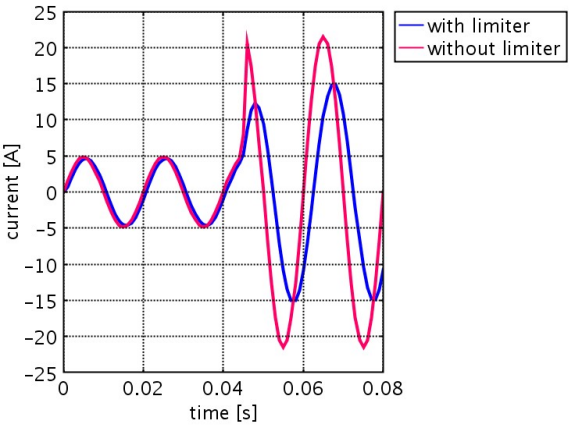

Figure 6.3: Current with and without limiter.

6.4.2 Constants, Functions and Subdomain and Global Expressions

Constants

Note that a fill-factor in the coils in **not** used as the expression for the induced voltage in scaling invariant for the induced voltage.

Functions Functions are used to define the different BH-curves.

Global expressions The flux variables and their derivatives are included to check the model. They are not used in the computation as such. Flux variables are used to verify whether or not the core legs are in saturation. The flux derivative variables are used to check the induced voltage.

$$
\begin{aligned}
Vline &= Vmax\sin(\omega t) && (6.1)\\
Rline &= Rpre-(Rpre-Rpost)*flc2hs(t-Tfault,Tsmooth) && (6.2)\\
Vind1 &= -\text{sign}(Jz)*acNt*lz/accross*Eint1 && (6.3)\\
Vind2 &= -\text{sign}(Jz)*acNt*lz/accross*Eint2 && (6.4)\\
Vind &= Vind1+Vind2 && (6.5)\\
Bavrg1 &= Bint1/crwleg && (6.6)\\
Bavrg2 &= Bint2/crwleg && (6.7)\\
fluxt1 &= -acNt*lz*Btint1 && (6.8)\\
fluxt2 &= -acNt*lz*Btint2 && (6.9)
\end{aligned}
$$

6.4.3 Integration Coupling Variables

We keep two variables for the induced voltage in order to be able to monitor them seperately. Subdomain integration coupling variables for the induced voltage

$$
\begin{aligned}
Eint1 &= \int_{accoil1} E_z\,d\Omega = \int_{accoil1}\frac{\partial A_z}{\partial t}\,d\Omega && (6.10)\\
Eint2 &= \int_{accoil2} E_z\,d\Omega = \int_{accoil2}\frac{\partial A_z}{\partial t}\,d\Omega && (6.11)
\end{aligned}
$$

Electrical constants	
ω	2 π 50
Vmax	28
Rpre	4.0
Rpost	0.1
Tfault	45e-3
Tsmooth	1e-3
Core	
lz (Length in z-direction)	25e-3
flcrwleg	crwleg
crcross (Core leg cross-section)	flcrwleg*lz
AC coil	
acNt (Number of turns)	200
accross (Cross-section)	accoilw*accoilh
Iac (Current value)	5
DC coil	
dcNt (Number of turns)	250
dccross (Cross-section)	dccoilw*dccoilh
Idc (Current value)	10
BH curve data	
linmurfe	1000
bha	2.12e-4
bhb	7.358
bhc	1.18e6
C_1	.25
C_2	.06

Table 6.1: Constants Used

and boundary integration coupling variables for the average flux and the time-derivative of the flux

$$Bint1 = \int_{fluxline1} B_y\, dl = \int_{fluxline1} -\frac{\partial A_z}{\partial x}\, dl \tag{6.12}$$

$$Bint2 = \int_{fluxline2} B_y\, dl = \int_{fluxline2} -\frac{\partial A_z}{\partial x}\, dl \tag{6.13}$$

$$Btint1 = \frac{d}{dt}\int_{fluxline1} B_y\, dl = \int_{fluxline1} -\frac{\partial^2 A_z}{\partial x\, \partial t}\, dl \tag{6.14}$$

$$Btint2 = \frac{d}{dt}\int_{fluxline2} B_y\, dl = \int_{fluxline2} -\frac{\partial^2 A_z}{\partial x\, \partial t}\, dl \tag{6.15}$$

where the minus sign in the expressions with index two take the direction of the current into account.

6.4.4 Application mode, subdomain and boundary settings

The magnetic field is modeled by a partial differential equation for the z-component of the magnetic vector potential A_z (perpendicular current model) satisfying the following equation

$$\sigma\frac{\partial A_z}{\partial t} + \frac{\partial}{\partial x}\big(\nu_0\,\nu_r(B)\frac{\partial A_z}{\partial x}\big) + \frac{\partial}{\partial y}\big(\nu_0\,\nu_r(B)\frac{\partial A_z}{\partial y}\big) = J_z(x,y,t) \tag{6.16}$$

where $\sigma = 0$ everywhere on Ω, supplied with boundary conditions. All time-dependency is thus in the current source! We do solve this equation with a time-stepping procedure as we need the derivative $\frac{\partial A_z}{\partial t}$ in defining the induced voltage.

- material characteristics:
  - ferromagnetic core: μ_r through BH-curve
  - coils and air: $\mu_r = 1$
- current exitation
  - DC coil: constant current density equal to $J_{z,dc} = \pm\frac{I_{dc,tot}}{S_{dc}} = \pm dcNt\frac{Idc}{dccross}$
  - AC coil: voltage driven by a sinusoidal voltage source $Vline$ through the circuit relation given below. The variable $Itot$ is to be computed such that $J_{z,ac} = \pm\frac{I_{ac,tot}}{accross} = \pm acNt\frac{Itot}{accross}$

Different Application Modes In different application modes we subsequently solve for

- the impedance using three different models
- the initial guess for the transient simulation
- the non-linear transient simulation including the fault

6.4.5 ODE Settings

The current in the AC coil is modeled by a crircuit relation (an ODE) for the variable I_{tot}

$$V_{tot} = V_{res} + V_{ind} \tag{6.17}$$

$$= RI_{tot} + Vind1 + Vind2 \tag{6.18}$$

6.4.6 Numerical Results

Discuss that

- this configuration is not able to limit the during during both periods.

6.5 Open-Core Configuration

1. geometry of the AC coil changes

6.6 Three-Leg Configuration

1. new geometry
2. DC coils opposite polarity, AC coils different polarity
3. in the computation of the inductance only *only* AC coil needs to be taken into account
4. new integration coupling variables
5. new ODE setting

6.6.1 Source file of the open core model

```
%  Model of two coils with pierced core
%  The german BH curve requires a DC current away from zero in order
%  to converge
   flclear fem fem0
   close all

   %..Set switches..
   bhswtch = 'hyperchord';

   %..Number of turns and current values
   %..The current in the AC coil is set to compute the inductance of the coil
   Idc  = 10;
   dcNt = 250;
   Iac  = 5;
   acNt = 200;

   %..Create geometery..
   %....Core....
   crwin  = 12.5e-3;
   crwout = 37.5e-3;
   crwleg = crwout - crwin;
   crhin  = 39e-3;
   crhout = 63e-3;
   rad    = 3e-3;
   core   = fillet(rect2(-crwout,crwout,-crhout,crhout),'radii',rad) - ...
                   rect2(-crwin,crwin,-crhin,crhin);
   %....Flux integration lines....
   fluxline1 = line1([-crwout,-crwin],[0,0]);
   fluxline2 = line1([crwin,crwout],[0,0]);
   %....AC coil....
   accoilw      = 10e-3; accoilh = 20e-3;
   xspacer      = 0e-3;
   accoilradin  = crwin+crwleg+xspacer; accoilradout = accoilradin+accoilw;
   accoil_right = rect2(accoilradin,accoilradout,-accoilh/2,accoilh/2);
   accoil       = accoil_right+move(accoil_right,-2*accoilradin-accoilw,0);
   %....DC coil....
   dccoilh      = 10e-3; dccoilw = crwin/2;
   dccoilradin  = (crhout-crhin)/2; dccoilradout = dccoilradin + dccoilh;
   dccoilyc     = crhin+(crhout-crhin)/2;
   dccoil_top   = rect2(-dccoilw/2,dccoilw/2,dccoilradin,dccoilradout);
   dccoil       = dccoil_top + move(dccoil_top,0,-2*dccoilradin-dccoilh);
   dccoil       = move(dccoil,0,dccoilyc);
   %....Air....
   xmax = 400e-3; ymax = 400e-3;
   air = rect2(-xmax, xmax, -ymax, ymax);
```

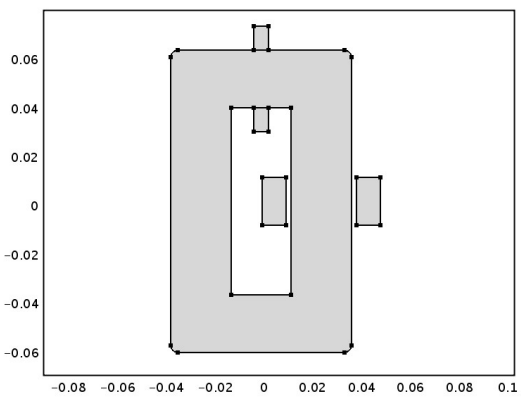

(a) Geometry

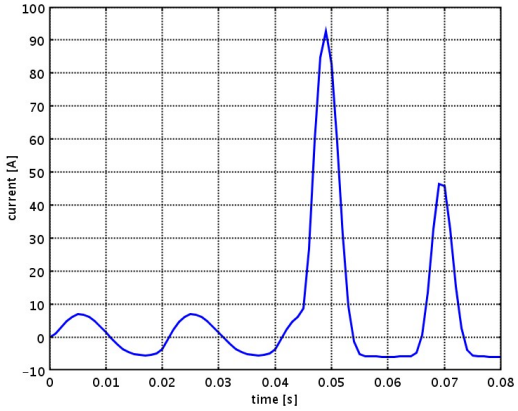

(b) Computed line current

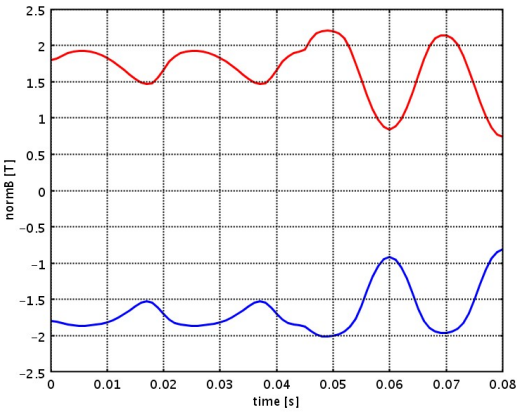

(c) Flux in left and right core leg

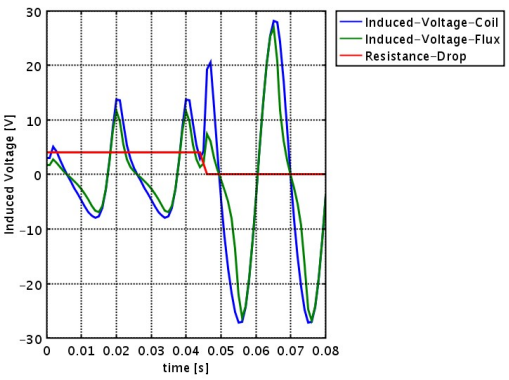

(d) Induced Voltage

Figure 6.4: Numerical results for the O-shaped core configuration.

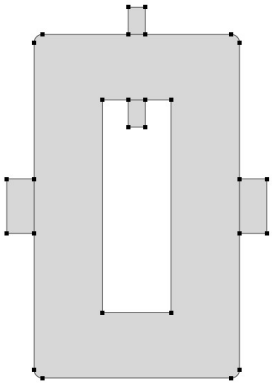

(a) Geometry

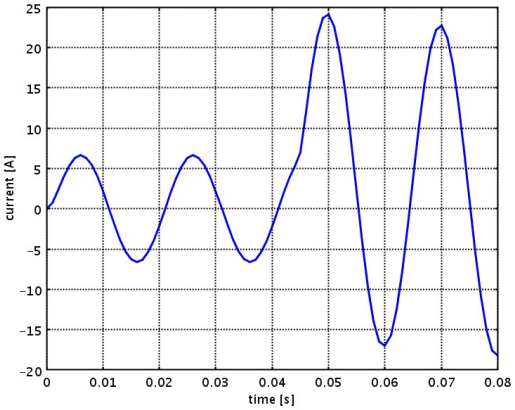

(b) Computed line current

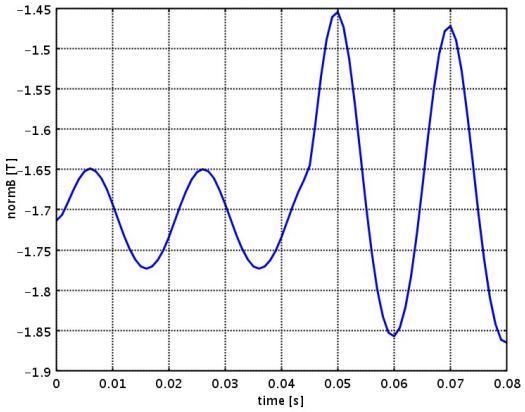

(c) Flux in left core leg

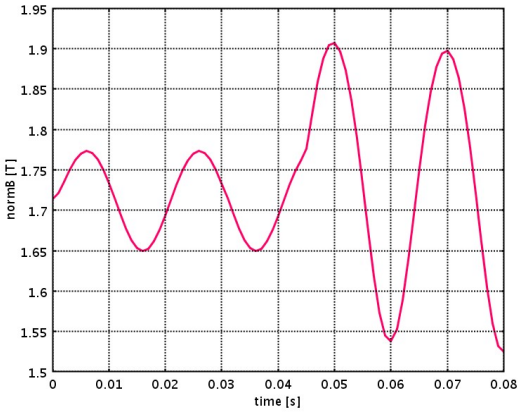

(d) Flux in right core leg

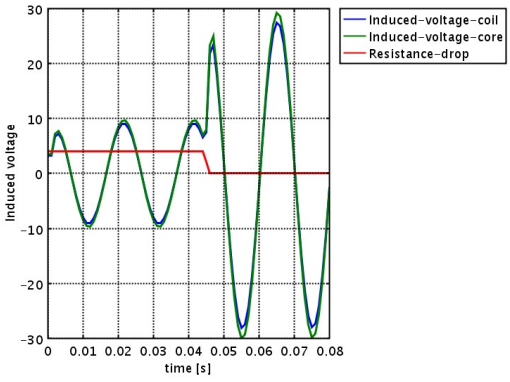

(e) Induced Votage

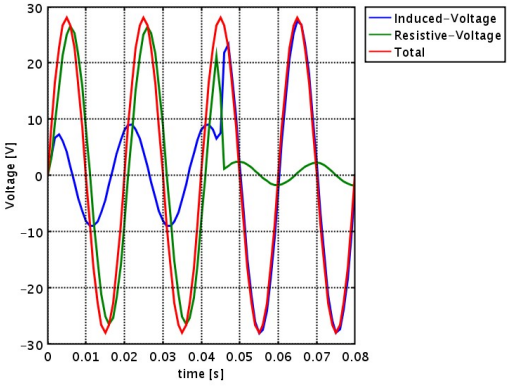

(f) Total Votage

Figure 6.5: Numerical results for the open-core configuration.

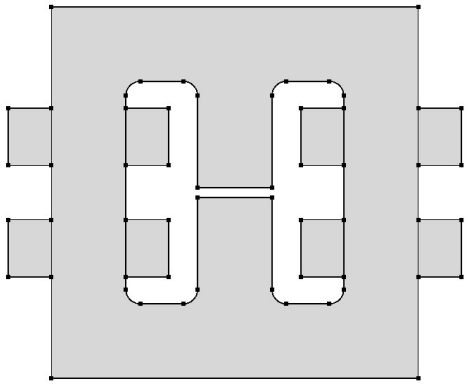

(a) Geometry

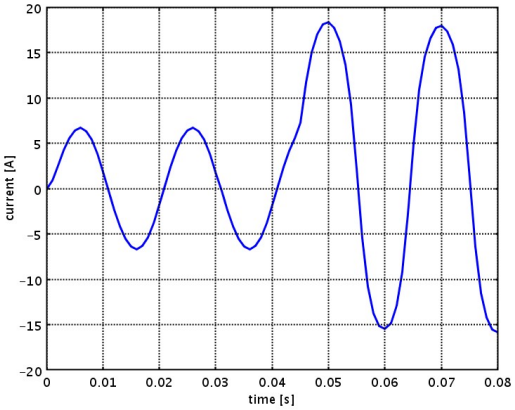

(b) Computed line current

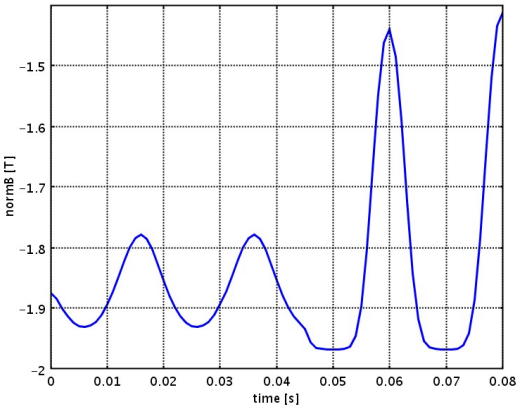

(c) Flux in left core leg

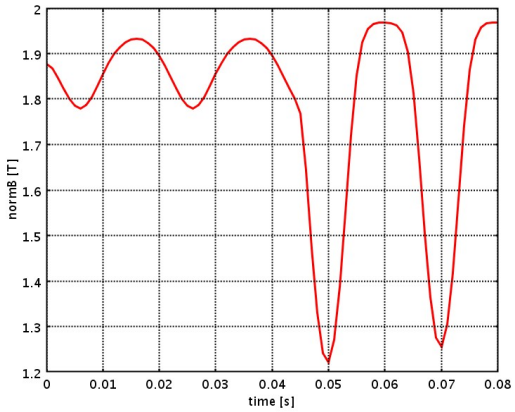

(d) Flux in right core leg

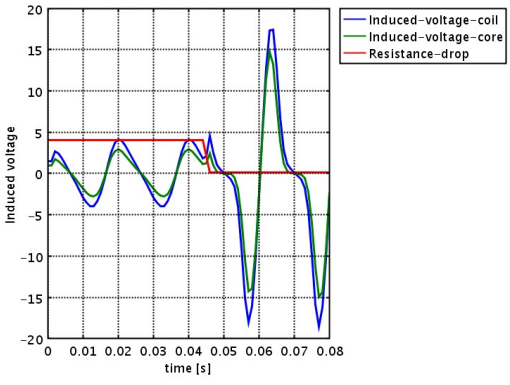

(e) Induced Votage in Left Core Leg

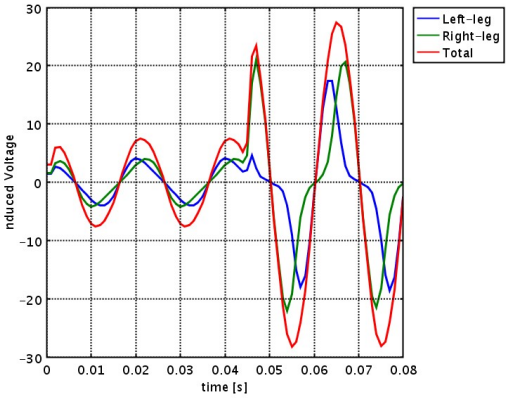

(f) Total Induced Votage

Figure 6.6: Numerical results for the three-legs configuration.

```
46
47  % Analyzed geometry
48  clear c s
49  c.objs={fluxline1,fluxline2};
50  c.name={'fluxline1','fluxline2'};
51  c.tags={'g5','g6'};
52
53  s.objs={air,accoil,dccoil,core};
54  s.name={'air1','accoil','dccoil','core'};
55  s.tags={'g1','g2','g3','g4'};
56
57  fem.draw=struct('c',c,'s',s);
58  fem.geom=geomcsg(fem);
59
60  %..Plot geometry..
61  if (0)
62    geomplot(fem,'edgelabels','on')
63    return
64  end
65
66  fem.const = {'om',              2*pi*50,...
67               'Vmax',            28,...
68               'Rpre',            4.0,...
69               'Rpost',           0.1,...
70               'Tfault',          45e-3,...
71               'Tsmooth',         1e-3,...
72               'lz',              50e-3,...
73               'flcrwleg',        crwleg,...
74               'crcross',         'lz*flcrwleg',...
75               'flacNt',          acNt,...
76               'accross',         accoilw*accoilh,...
77               'flIac',           Iac,...
78               'fldcNt',          dcNt,...
79               'flIdc',           Idc,...
80               'dccross',         dccoilw*dccoilh,...
81               'linmurfe',        '1000',...
82               'bha',             '2.12e-4',...
83               'bhb',             '7.358',...
84               'bhc',             '1.18e6',...
85               'C1',              '.25',...
86               'C2',              '.06'};
87
88  % Functions
89  clear fcns
90  fcns{1}.type='inline';
91  fcns{1}.name='rational(x,bha,bhb,bhc)';
92  fcns{1}.expr='1/(bha+(1-bha)*x^bhb/(x^bhb+bhc))';
93  fcns{1}.dexpr={'diff(1/(bha+(1-bha)*x^bhb/(x^bhb+bhc)),x)',...
94                 '0','0','0'};
95  fcns{2}.type='inline';
96  fcns{2}.name='hyperchord(x,C1,C2)';
97  fcns{2}.expr='C2*x/(4*pi*1e-7*sinh(x/C1))';
98  fcns{2}.dexpr={'diff(C2*x/(4*pi*1e-7*sinh(x/C1)),x)','0','0'};
99  fcns{3}.type='interp';
100 fcns{3}.name='bmurtabular';
101 fcns{3}.method='linear';
102 fcns{3}.extmethod='const';
103 fcns{3}.filename='/mnt/dutita1/nw/domenico/software/bh_curve/mur_normb_data.txt';
```

```
  fem.functions = fcns;

  % Global expressions
  fem.globalexpr = {'Vline',      'Vmax*sin(om*t)',...
                    'Vind1',      'flacNt*lz/accross*Eint1',...
                    'Vind2',      'flacNt*lz/accross*Eint2',...
                    'Vind',       'Vind1+Vind2',...
                    'Bavrg1',     'Bint1/flcrwleg',...
                    'Bavrg2',     'Bint2/flcrwleg',...
                    'fluxt1',     'flacNt*lz*Btint1',...
                    'fluxt2',     'flacNt*lz*Btint2',...
                    'Rline',      'Rpre - (Rpre-Rpost)*flc2hs(t-Tfault,Tsmooth)'};

  % Initialize mesh
  fem.mesh=meshinit(fem);
%% fem.mesh = meshrefine(fem);
%% fem.mesh = meshrefine(fem);

   if (0)
     meshplot(fem)
     return
   end

%%%%%%%%%%%%%%%%%%%%%%%%%%%%%%%%%%%%%%%%%%%%%%%%%%%%%%%%%%%%%%%%%%%%%%%%%%%%%%%%

  % Application mode 0: nominal current computation
  if (0)
    clear appl
    appl.mode.class = 'PerpendicularCurrents';
    appl.module = 'ACDC';
    clear bnd
    bnd.type = {'A0','cont'};
    bnd.ind = {[1,2,3,38],[4:37,39:41]};
    appl.bnd = bnd;
    clear equ
    equ.init = {'1e-6*sqrt(x^2+y^2)',0,0,0,0,0};
    if (strcmp(bhswtch,'linear')==1)
      equ.mur = {'linmurfe',1,1,1,1,1};
    elseif (strcmp(bhswtch,'rational')==1)
      equ.mur = {'rational(normB,bha,2*bhb,bhc)',1,1,1,1,1};
    elseif (strcmp(bhswtch,'hyperchord')==1)
      equ.mur = {'hyperchord(normB,C1,C2)',1,1,1,1,1};
    elseif (strcmp(bhswtch,'tabular')==1)
      equ.mur = {'bmurtabular(normB)',1,1,1,1,1};
    else
      error('  error:: undefined BH switch')
    end
        equ.Jez = {0,'-flacNt*flIac/accross','flacNt*flIac/accross',0,0,0};
    equ.ind = {[3,4],2,8,6,7,[1,5]};
    appl.equ = equ;
    fem.appl{1} = appl;
    fem.frame = {'ref'};
    fem.border = 1;
    clear units;
    units.basesystem = 'SI';
    fem.units = units;

    % ODE Settings
```

```
    clear ode
    ode.dim={'Itot'};
    ode.f={'0'};
    ode.init={'0'};
    ode.dinit={'0'};
    fem.ode=ode;

    % Multiphysics
    fem=multiphysics(fem);

    % Extend mesh
    fem.xmesh=meshextend(fem);

    % Solve problem
    fem.sol=femstatic(fem, ...
                      'solcomp',{'Az'}, ...
                      'outcomp',{'Az'});

    Rpre  = 4; Rpost = .1; om = 2*pi*50; Vmax = 28; lz = 25e-3;
    Wmtot = lz*postint(fem,'.5*Bx*Hx+.5*By*Hy','Edim',2,'Dl',[1:8]);
    L     = 2*Wmtot /Iac^2;
    Xpre  = sqrt(Rpre^2  + om^2*L^2); Ipre = Vmax/Xpre;
    Xpost = sqrt(Rpost^2 + om^2*L^2); Ipost = Vmax/Xpost;
    fprintf('  The inductance of the coil   = %f H. \n', L)
    fprintf('  Nominal current before fault = %f Amp. \n', Ipre)
    fprintf('  Nominal current after  fault = %f Amp. \n', Ipost)

    return

  end %..Nominal current computation

%%%%%%%%%%%%%%%%%%%%%%%%%%%%%%%%%%%%%%%%%%%%%%%%%%%%%%%%%%%%%%%%%%%%%%%%%%%%%%%%%%%%

  % Application mode 1: generating initial guess for the DC coil flux
  if (1)
    clear appl
    appl.mode.class = 'PerpendicularCurrents';
    appl.module = 'ACDC';
    clear bnd
    bnd.type = {'A0','cont'};
    bnd.ind = {[1,2,3,38],[4:37,39:41]};
    appl.bnd = bnd;
    clear equ
    equ.mur = {'100',1,1,1,1,1};
    equ.Jez = {0,0,0,'fldcNt*flIdc/dccross',...
               '-fldcNt*flIdc/dccross',0};
    equ.ind = {[3,4],2,8,6,7,[1,5]};
    appl.equ = equ;
    fem.appl{1} = appl;
    fem.frame = {'ref'};
    fem.border = 1;
    clear units;
    units.basesystem = 'SI';
    fem.units = units;

    % ODE Settings
    clear ode
    ode.dim={'Itot'};
```

```
    ode.f={'0'};
    ode.init={'0'};
    ode.dinit={'0'};
    fem.ode=ode;

    % Multiphysics
    fem=multiphysics(fem);

    % Extend mesh
    fem.xmesh=meshextend(fem);

    % Solve problem
    fprintf('  Generating initial guess for the DC coil flux ...\n')
    fem.sol=femstatic(fem, ...
                      'solcomp',{'Az'}, ...
                      'outcomp',{'Az','Itot'});
    fprintf('  ... done! \n')

    fem0 = fem;


  end %.. Parametric solver in DC winding

%%%%%%%%%%%%%%%%%%%%%%%%%%%%%%%%%%%%%%%%%%%%%%%%%%%%%%%%%%%%%%%%%%%%%%%%%%%%%%%%%%

  % Application mode 2: generating initial guess for the AC coil flux
  if (1)
    clear appl
    appl.mode.class = 'PerpendicularCurrents';
    appl.module = 'ACDC';
    clear bnd
    bnd.type = {'A0','cont'};
    bnd.ind = {[1,2,3,38],[4:37,39:41]};
    appl.bnd = bnd;
    clear equ
    if (strcmp(bhswtch,'linear')==1)
      equ.mur = {'linmurfe',1,1,1,1,1};
    elseif (strcmp(bhswtch,'rational')==1)
      equ.mur = {'rational(normB,bha,2*bhb,bhc)',1,1,1,1,1};
    elseif (strcmp(bhswtch,'hyperchord')==1)
      equ.mur = {'hyperchord(normB,C1,C2)',1,1,1,1,1};
    elseif (strcmp(bhswtch,'tabular')==1)
      equ.mur = {'bmurtabular(normB)',1,1,1,1,1};
    else
      error('  error:: undefined BH switch')
    end
    equ.Jez = {0,0,0,'fldcNt*flIdc/dccross',...
               '-fldcNt*flIdc/dccross',0};
    equ.ind = {[3,4],2,8,6,7,[1,5]};
    appl.equ = equ;
    fem.appl{1} = appl;
    fem.frame = {'ref'};
    fem.border = 1;
    clear units;
    units.basesystem = 'SI';
    fem.units = units;

    % ODE Settings
```

```
      clear ode
      ode.dim={'Itot'};
      ode.f={'0'};
      ode.init={'0'};
      ode.dinit={'0'};
      fem.ode=ode;

      % Multiphysics
      fem=multiphysics(fem);

      % Extend mesh
      fem.xmesh=meshextend(fem);

      % Solve problem
      fprintf('  Generating initial guess for the DC coil flux ...\n')
      fem.sol=femstatic(fem, ...
                         'init', fem0.sol,...
                         'solcomp',{'Az'}, ...
                         'outcomp',{'Az','Itot'}, ...
                         'Pname','flIdc',...
                         'Plist',[Idc],...
                         'Maxiter',40,...
                         'Ntol',1e-8);
      fprintf('   ... done! \n')

      fem0 = fem;

    end %.. Generatring initial guess for the AC flux

%%%%%%%%%%%%%%%%%%%%%%%%%%%%%%%%%%%%%%%%%%%%%%%%%%%%%%%%%%%%%%%%%%%%%%%%%%%%%%%%%

    % Application mode 3: transient simulation
    % Saturation current in the DC winding
    % ODE solution in the AC winding

    clear appl
    appl.mode.class = 'PerpendicularCurrents';
    appl.module = 'ACDC';
    clear prop
    prop.analysis='transient';
    appl.prop = prop;
    clear bnd
    bnd.type = {'A0','cont'};
    bnd.ind = {[1,2,3,38],[4:37,39:41]};
    appl.bnd = bnd;
    clear equ
    equ.init = {'1e-6*sqrt(x^2+y^2)',0,0,0,0,0};
    if (strcmp(bhswtch,'linear')==1)
      equ.mur = {'linmurfe',1,1,1,1,1};
    elseif (strcmp(bhswtch,'rational')==1)
      equ.mur = {'rational(normB,bha,2*bhb,bhc)',1,1,1,1,1};
    elseif (strcmp(bhswtch,'hyperchord')==1)
      equ.mur = {'hyperchord(normB,C1,C2)',1,1,1,1,1};
    elseif (strcmp(bhswtch,'tabular')==1)
      equ.mur = {'bmurtabular(normB)',1,1,1,1,1};
    else
      error('  error:: undefined BH switch')
    end
```

```
336     equ.Jez = {0,'flacNt*Itot/accross','-flacNt*Itot/accross',...
337                'fldcNt*flIdc/dccross','-fldcNt*flIdc/dccross',0};
338     equ.ind = {[3,4],2,8,6,7,[1,5]};
339     appl.equ = equ;
340     fem.appl{1} = appl;
341     fem.frame = {'ref'};
342     fem.border = 1;
343     clear units;
344     units.basesystem = 'SI';
345     fem.units = units;
346
347     % Coupling variable elements
348     clear elemcpl
349     % Integration coupling variables
350     clear elem
351     elem.elem = 'elcplscalar';
352     elem.g = {'1'};
353     src = cell(1,1);
354     clear bnd
355     bnd.expr = {{{},{},'By',{},{},{}},{{},{},{},{},'By',{}},{{},{},'-Azxt',{}, ...
356       {},{}},{{},{},{},{},'-Azxt',{}},{},{}};
357     bnd.ipoints = {{{},'4','4',{},{},{}},{{},{},{},'4','4',{}},{{},'4','4',{},{}, ...
358       {}},{{},'4',{},'4','4',{}},{},{}};
359     bnd.frame = {{{},'ref','ref',{},{},'ref'},{{},{},{},'ref','ref','ref'},{{}, ...
360       'ref','ref',{},{},'ref'},{{},'ref',{},'ref','ref','ref'},{},{}};
361     bnd.ind = {{'1','2','3','4','5','7','8','9','11','12','13','14','15', ...
362       '16','17','18','19','20','21','22','23','24','25','26','27','28','31', ...
363       '32','33','34','35','36','37','38','39','40'},{'6'},{'10'},{'29'},{'30'}, ...
364       {'41','42'}};
365     clear equ
366     equ.expr = {{},{},{},{},{{},'-Ez',{},{}},{{},{},{},'Ez'}};
367     equ.ipoints = {{},{},{},{},{{},'4','4',{}},{{},{},{},'4'}};
368     equ.frame = {{},{},{},{},{{},'ref','ref','ref'},{{},{},'ref','ref'}};
369     equ.ind = {{'1','3','4','5','6'},{'2'},{'7'},{'8'}};
370     src{1} = {{},bnd,equ};
371     elem.src = src;
372     geomdim = cell(1,1);
373     geomdim{1} = {};
374     elem.geomdim = geomdim;
375     elem.var = {'Bint1','Bint2','Btint1','Btint2','Eint1','Eint2'};
376     elem.global = {'1','2','3','4','5','6'};
377     elem.maxvars = {};
378     elemcpl{1} = elem;
379     fem.elemcpl = elemcpl;
380
381     % ODE Settings
382     clear ode
383     ode.dim={'Itot'};
384     ode.f={'Rline*Itot+Vind-Vline'};
385     ode.init={'0'};
386     ode.dinit={'0'};
387     fem.ode=ode;
388
389     % Multiphysics
390     fem=multiphysics(fem);
391
392     % Extend mesh
393     fem.xmesh=meshextend(fem);
```

```
394
395 % Solve problem
396 fem.sol=femtime(fem, ...
397                 'init', fem0.sol,...
398                 'solcomp',{'Az','Itot'}, ...
399                 'outcomp',{'Az','Itot'}, ...
400                 'atol',1e-6,...
401                 'rtol',1e-6,...
402                 'tlist',[0:0.001:0.08], ...
403                 'tout','tlist',...
404                 'nlsolver','manual', ...
405                 'ntolfact',0.01, ...
406                 'maxiter',25, ...
407                 'dtech','const', ...
408                 'damp',1.0, ...
409                 'jtech','minimal',...
410                 'linsolver','pardiso', ...
411                 'errorchk','off');
412
413 % Plot current
414 postglobalplot(fem,'Itot')
415 postglobalplot(fem,{'Bavrg1','Bavrg2'})
416 postglobalplot(fem,{'Vind1+Vind2','fluxt1+fluxt2'})
417 postglobalplot(fem,'Itot')
```

Chapter 7

Three Dimensional FE Models of Inductive Fault Current Limiters

To do

- add references to De Gersem and Dular on the field circuit coupling

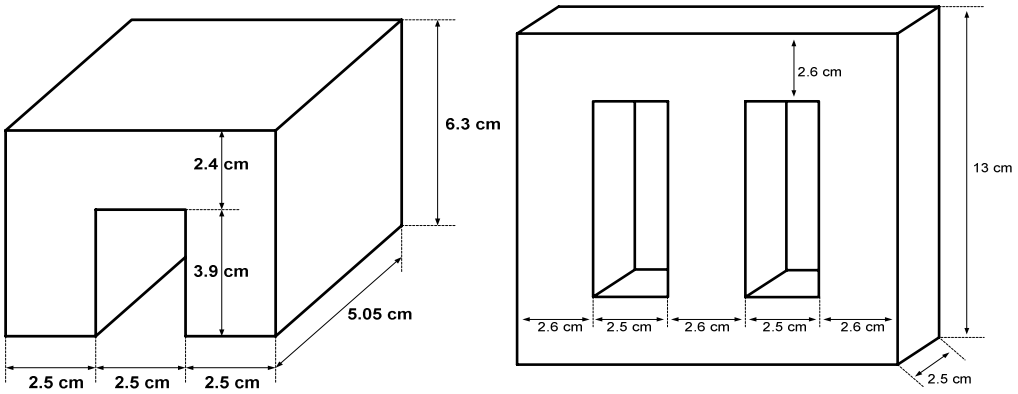

(a) Open core (b) Three-leg four winding

Figure 7.1: Geometries studied

7.1 Open-Core Configuration

7.1.1 Geometry

In defining the geometry, the core acts as *master*, while the DC and AC coil act as slave. The geometry will consist of the following four parts:

1. **the core**: build by extruding a working plane in the yz-plane in the x-direction. There will be a relation between the depth and width of the core leg.

   (a) core variables

   ```
   crlegw = ;
   crwin = ; crwout = crwin + crlegw;
   crhout = ; crhin = ;
   crd = ;
   ```

   (b) core working plane:

   ```
   core_plane = fillet(rect2(-crwout,crwout,-crhout, crhout), 'rad', rad) ...
                        - fillet(rect2(crwin,crwin,-crhin,crhin), 'rad', rad);
   ```

(c) core extrusion

```
set working plane at x = 0
core = extrude(core_plane, 'distance', 2*crd);
```

2. **flux integration surfaces**:
3. **the generic coil**: build by extruding a working plane in the xy-plane in the z-direction
   (a) generic coil variables

```
coilw = ; coilh = ;
yspacer = ;  zspacer = ;
coilradin = crlegw/2+yspacer; coilradout = coilradin+coilw;
coilyc = crwin+crwleg/2; coilzc= coilh/2 + zspacer;
```

   (b) coil working plane:

```
coil_plane = circ2(coilradout) - circ2(coilradin);
```

   (c) coil extrusion

```
set working plane at z = 0
coil = extrude(coil_plane, 'distance', coilh)
```

4. **the DC coil**: by moving the generic coil in positive y-direction and in positive z-direction
   (a) DC coil variable

```
dccoilzc= coilh/2 + zspacer;
```

   (b) `dccoil = move(coil,0,coilyc,dccoilzc);`
5. **the AC coil**: by moving the generic coil in positive y-direction and in negative z-direction
   (a) AC coil variable

```
accoilzc= -coilh/2 - zspacer;
```

   (b) `accoil = move(coil,0,coilyc,accoilzc);`
6. **the air**: build using the `block3` command

For the ease of modification of this geometry we will work with a full model.

7.1.2 Meshing

Currently the meshing happens fully automatically, excepts for the option `hauto` used in `meshinit`. Due to this automation, difficulties may occur in case the space between the coils and the core leg is to small. This issue will have to be dealt with in the future.

7.1.3 Constants, Functions and Subdomain and Global Expressions

Constants

Note that a fill-factor in the coils in **not** used

Functions

Here we define the BH curves and the winding functions.

Subdomain expressions

Here we define the densities for the induced voltage

Global expressions

Here we define the electrical excitation and the induced voltage.

Electrical constants	
ω	$2\ \pi\ 50$
DC coil	
Number of turns Cross-section Current value	
AC coil	
Number of turns Cross-section	
BH curve data	
a b c C_1 C_2	2.12e-4 7.358 1.18e6 .25 .06

Table 7.1: Constants Used

7.1.4 Application modes

We solve for both the vector and scalar potential. The scalar potential is used to avoid that during time integration components in the null space of the curl-curl operator are introduced.

7.1.5 Integration coupling variables

Here we integrate the induced voltage density to obtain the total induced voltage.

7.1.6 Definition of the ODE

The sum of resistive and induced voltage is at all times equal to the total applied voltage.

7.1.7 Solution process

7.1.8 Post processing

7.2 Different solution modes

7.2.1 Linear core

7.2.2 Non-linear core

Define the different stages.

Chapter 8

Size Optimization

1. zeroth order model by Dalibor: number of winding determines the Ohmic losses. These losses should not exceed an a-priori established limit. This is guaranteed by imposing the number of turns. From this number of turns and from the value of the applied voltage, normB and by using the analyical expressions for the impedance and the induced voltage, an estimate of the leg cross-section, and thus the leg width can be establised.

2. formulation of the sizing optimization (later extend to topology optimization) problem
(in the order in which we intend to solve the problem):

   (a) minimize mass subject to sufficient current limiting capabilities. This limiting capability can be set equal to the one of the initial configuration.

   (b) maximize current limiting capabilities subject to a constraint on the mass (same remark as in previous case)

   (c) multi-objective optimization problem with mass and limiting capability as conflicting objectives: compute the Pareto-front (can be done easily using an analytical model)

3. design variables and box constraints: we first consider the sizes of the core as design variables. In the design, the vertical and horizontal core leg width should remain equal. We therefore have four design variables: the half inner window width and height (cr_w_in and cr_h_in), the depth (cr_d) and core leg width (cr_leg_w). The lower bounds on the first two variables should be such to leave sufficient space for the dc coil. In a first analysis the size of the inner window and the core depth can be taken to constant. In a second analysis we can allow the height of the inner window to change. We observe that changing the width of the window implies more material for the AC coil. The same is not true for changes in the height.
Experiments by Dalibor indicate that for the current limiting capability is most sensitive to the cross-section of the core legs and the number of turns in the ac coil.
In a later stage we will add dimensions of the ac and dc coil as design variables and number of turns of the coil (mixed integer problem).

4. computation of the objectives: for the computation of the mass we use

$$\begin{aligned} \text{core-mass} &= \rho\, cr\_d\,[2(cr\_h\_in + cr\_leg\_w)\cdot 2(cr\_w\_in + cr\_leg\_w) - 2cr\_h\_in\cdot 2cr\_w\_in)] \quad (8.1)\\ &= \rho\, cr\_d\,[4cr\_leg\_w\cdot(cr\_h\_in + cr\_h\_in + cr\_leg\_w)]\,; \quad (8.2)\end{aligned}$$

   for the computation of the current limiting capability or induced voltage V_{ind} we will for time being consider a time-harmonic computation ($\frac{d}{dt}\rightarrow j\omega$) of the post-fault situation. Doing so we do **not** take the peak current into account. We have that

$$I = \text{Re}[\widehat{I}\exp(j\omega t)]\,, \quad (8.3)$$

   and solve for $\widehat{I}$. We consider the following three models of increasing complexity:

   (a) analytical model. One of the difficulties in the analytical model is the correct estimation of the flux path.

We have that

$$\begin{aligned} V_{ind} &= \frac{d}{dt}(L\,I) && (8.4)\\ &= j\omega L\,I && (8.5)\\ &= j\omega\mu_r\mu_0 N_{ac}^2 \frac{A_c}{l}\,I && (8.6)\\ &= 2\,\pi\,j\,f\mu_r\mu_0 N_{ac}^2 \frac{cr\_leg\_w \cdot cr\_d}{l} I\,, && (8.7) \end{aligned}$$

where l denotes the length of the flux path. This means that the induced voltage lags the current by $\pi/2$ and its amplitude is function of the design variables. In a classical ac core layout, one could put

$$l = 2(cr\_h\_in + cr\_w\_in + cr\_w\_leg) \tag{8.8}$$

For the open-core a more appropriate expression for the flux path could be

$$l = C \cdot cr\_h\_in \tag{8.9}$$

where $C > 1$ is a constant to be determined.

(b) 2D and 3D time-harmonic FEM model. In this model we have

$$V_{ind} = N_{ac}\frac{d}{dt}\int_{S_{cr}} B_y d\Omega = j\omega N_{ac}\int_{S_{cr}} B_y d\Omega = V_{ind,1} - V_{ind,2}\,, \tag{8.10}$$

where

$$V_{ind,i} = \frac{N_{ac}\,\ell_z}{S_{cl,i}}\int_{S_{cl,i}} E_z d\Omega = j\omega\frac{N_{ac}\,\ell_z}{S_{cl,i}}\int_{S_{cl,i}} A_z d\Omega\,. \tag{8.11}$$

5. initial configuration and objective values:

parameter	notation	value	units
mass density core	ρ	7850	kg/m^3
number of AC turns	N_{ac}	100	-

Table 8.1: parameter values

cr_w_in	xxx [mm]	core-mass	xxx [kg]
cr_h_in	xxx [mm]	V_{ind}	xxx [V]
cr_leg_w	xxx [mm]		
cr_d	xxx [mm]		

Table 8.2: Initial configuration and objective values.

6. coarse model (analytical) design problem and solution techniques: in case we set out to minimize the mass, we obtain:
find $x^* \in X$ such that:

$$x^* = \text{argmin}_{x\in X}\text{core-mass}(x) \quad \text{such that} \quad V_{ind}(x) \geq V_{ind,0} \tag{8.12}$$

By incorporating the constraint on the induced voltage in the definition of the design space space, we can formulate this as
find $x^* \in \overline{X}$ such that:

$$x^* = \text{argmin}_{x\in \overline{X}}\text{core-mass}(x) \tag{8.13}$$

We intend to solve this problem using the Nelder-Mead simplex method and a gradient based optimization algorithm with exact gradients with multiple starting points. Can the latter be done in Maple?

7. Pareto front: generate the coarse model Pareto front using a brute force approach (4-fold loop in the design space).

8. space mapping optimization: identity mapping on the mass, constraint mapping on the induced voltage.

9. work in stages: Pareto front for analytical model (Dalibor?), build 2D time-harmonic FEM (Domenico), Pareto front for 2D FEM model, build space-mapping function via a least-squares procedure, Pareto front for mapped coarse model and comparison with FEM model, extend to 3D FEM, extend from time-harmonic to transient.

Bibliography

[1] Donald E. Knuth. Safety Transformer Mofdel. Technical Report STAN-CS-83-980, Department of Computer Science, Stanford University, Stanford, CA 94305, September 1983.

[2] Donald E. Knuth. Safety Transformer Mofdel. Technical Report STAN-CS-83-980, Department of Computer Science, Stanford University, Stanford, CA 94305, September 1983.